A TOPOLOGY–BASED MODEL FOR TWO-WINDING, SHELL-TYPE, SINGLE-PHASE TRANSFORMER INTER-TURN FAULTS.

A Thesis

Presented in Partial Fulfillment of the Requirements for the

Degree of Master of Science

with a

Major in Electrical Engineering

in the

College of Graduate Studies

University of Idaho

by

Liman Zhuang

December 2014

Major Professor: Brian Johnson, Ph.D.

AUTHORIZATION TO SUBMIT THESIS

This thesis of Liman Zhuang for the degree of Master of Science with a Major in Electrical Engineering and titled "A TOPOLOGY–BASED MODEL FOR TWO-WINDING, SHELL-TYPE, SINGLE-PHASE TRANSFORMER INTER-TURN FAULTS" has been reviewed in final form. Permission, as indicated by the signatures and dates below, is now granted to submit final copies to the College of Graduate Studies for approval.

Major Professor:

_____Date_____

Brian Johnson, Ph.D.

Committee

Members: _____Date_____

Richard Wall, Ph.D.

_____Date_____

Joe Law, Ph.D.

Department

Administrator: _____Date_____

Fred Barlow, Ph.D.

Discipline's

College Dean:

_____Date_____

Larry Stauffer, Ph.D.

Final Approval and Acceptance:

Dean of the College

Of Graduate Studies: _____Date_____

Jie Chen, Ph.D.

ABSTRACT

This thesis develop a topology-based model for two-winding, shell-type, single-phase transformer inter-turn faults. The principle of duality between the electric and magnetic equivalent circuits is concisely explained. The magnetic equivalent circuit of a two-winding, shell-type, single-phase transformer is extended to that of the magnetic circuit with an inter-turn fault. The model is implemented in the Alternative Transients Program (ATP/EMTP) using ATP components. The model is verified by Professor Mork's 150kVA three-phase transformer and Professor Johnson's 55kVA three-phase transformer. While the developed model is for single-phase transformers, extending it to topology-based, three-phase, three-legged and five-legged transformers are straight forward. Based on basic electric theory, the thesis also derived equations for direct solution of the transformer inter-turn fault. This may find usage in transformer relay protection. The thesis discusses using PSPICE for the solution of transformer inter-turn fault as well.

ACKNOWLEDGMENTS

I would like to express my sincere gratitude to my advisor Prof. Brian Johnson for the continuous support of my Master study and research, for his patience, motivation, enthusiasm, and immense knowledge. His guidance and encouragement helped me in all the time of research and writing of this thesis. I could not have imagined having a better advisor and mentor for my Master study.

Besides my advisor, I would like to thank the rest of my thesis committee: Prof. Richard Wall and Prof. Joe Law, for their valuable input, insightful comments, questions, and advice reviewing my thesis.

Last but not least, a special thanks to my family for their support and love. Words cannot express how grateful I am to my husband and my two daughters, for their encouragement and patience in all the difficult times.

TABLE OF CONTENTS

LIST OF FIGURES

LIST OF TABLES

ACRONYMS

ATP	----	Alternative Transients Program
EMTP	----	Electromagnetic Transients Program
HV	----	High Voltage
LV	----	Low Voltage
mmf	----	Magnetomotive force
FPGA	----	Field Programmable Gate Array
PSPICE	----	Personal Computer Simulation Program with Integrated Circuit Emphasis
ABM	----	Analog Behavioral Modeling
FEM	----	Finite Element Method

CHAPTER 1: INTRODUCTION

Power transformers are important components of the electric energy transmission and distribution system for electric utilities. In view of the increased demand for reliable and high quality energy supply, electric utilities are more interested in evaluating incipient transformer failures. The inter-turn winding faults, occurring primarily from turn-to-turn insulation degradation, are one of the leading causes of failures in power transformers. Early stages of winding inter-turn faults may often have negligible effects on the transformer performance; however, such faults may rapidly lead to more serious forms of faults: phase-to-ground or phase-to-phase faults. While the circulating current in the faulted turns is large, the currents in the terminals of the transformer are much smaller, which causes difficulty in the early detection of the inter-turn faults. It would be advantageous to detect an inter-turn fault in its earliest stage while the transformer is in operation to prevent further damages to the transformer thereby reducing repair cost and transformer outage time.

There have been many investigations of inter-turn faults in power transformers. Most of them concentrated on modeling inter-turn faults. To explore the inter-turn faults, custom-built transformer models have been built and tested extensively; several simulation methods have been published. The most widely known transformer model of inter-turn faults is given in the paper written by Bastard et al, which is based on an electric equivalent circuit model [1, 2]. Another group of authors proposed using a magnetic circuit to analyze the transformer inter-turn faults [3, 4, 5]. The third group of authors used the finite-element method to solve the inter-turn fault problem [6]. The fourth group of researchers built a scale model transformer and experimented on it [7]. It is reported that the existing methods for detecting inter-turn faults on energized transformers are not always accurate or reliable, in fact, due to weaknesses in models [7].

Bastard's paper derived the resistance and inductance models which are entirely compatible with the Electromagnetic Transients Program (EMPT) [1]. EMTP subroutine BCTRAN represents a two-winding, three-phase transformer as a 6 x 6 resistance matrix and a 6 x 6 inductance matrix. When inter-turn fault occurred on one of the windings, the dimension of

the *R* and *L* matrices is extended to 8 x 8, by using the three principles: consistency, leakage, and proportionality. Implementation of the proposed method assumes the knowledge of evaluating the leakage factors between the various coils of the transformer, which in turn needs transformer design data, unfortunately it is usually hard to obtain. The method is valid only for linear operation of the transformer.

M. Jabloński's paper uses the analytical method to calculate the transformer response to an inter-turn fault [2]. The paper deals with internal faults in large power transformers. The explanation of such faults is followed by the description of an analytical method proposed for the calculation of the power flow during an inter-turn fault, including the current supplied by the power grid, the current in a group of short-circuited turns, and the current in the fault location. The paper gives a clear and straightforward description of the process of the inter-turn faults: it usually occurs in one phase of the high voltage (HV) side, and initially involves a small number of turns, for example, one or two turns. Faults can be created either by direct contact or by an electric arc, which can burn in either a stable or an intermittent way. Each of these two fault types can transform into the other. After the arc has been extinguished, and neither conditions for its re-ignition exist nor direct contact is re-established, the inter-turn fault disappears, leaving, however, the local insulation damaged so that even a slight overvoltage or a dynamic stress suffices to repeat the short-circuit and complete the damage. Most inter-turn faults constitute a serious immediate threat.

Oliveira's paper investigates the behavior of power transformers under the occurrence of permanent or intermittent winding insulation faults [3]. For the study of these phenomena, a simple and efficient permeance-based electromagnetic transformer model is proposed, which is based on the simultaneous consideration of magnetic and electric equivalent circuits. To incorporate the internal faults in this model, a suitable equivalent circuit of the faulty winding is described. Experimental and simulation tests results are presented in this paper, which demonstrate not only the adequacy of the digital transformer model for winding fault studies, but also the effectiveness of the proposed technique for detecting winding inter-turn insulation faults in three-phase transformers under load.

J. R. Espinoza's paper presents a model corresponding to an aging fault with the sequential electrical arc fault [4]. The main contribution of the paper is the derivation of the inverse inductance matrix for the transformer inter-turn fault.

Professor Mork stated that an important aspect to investigate when designing transformer protection schemes is the protection against internal fault [5]. Although the accurate modeling and simulation of internal faults can be an important tool for protection engineers, there is presently no transformer model in ATP with this capability. This paper investigates on the development of transformer winding fault models based on two different sources of information: 1) test-report data and 2) design information. Simulation results are compared to laboratory measurements and conclusions regarding their accuracy are given. Relevant work in this area is focused on building internal fault models for EMTP based on rules of consistency, leakage, and proportionality applied to the faulted winding sections. The method has the drawback of resorting to empirical correction factors that decrease the accuracy of the model whenever winding sections of irregular geometry are encountered or when small sections that do not reach full window height must be studied. This problem can be avoided through the development of transformer models based on the Finite Element Method (FEM). FEM may be the most accurate approach for this purpose but it requires the knowledge of detailed design information that in most cases is not readily available. A model built from only factory test-report information can be a practical alternative but its accuracy is unknown. The paper describes some practical methods for modeling internal faults according to the type of problem and amount of information available with the objective of creating a suitable model for ATP in any cases.

Wang's paper presents a methodology to model internal incipient winding faults in distribution transformers [6]. The models were implemented by combining deteriorating insulation models with an internal short circuit fault model. The internal short circuit fault model was developed using the FEM. The deteriorating insulation model, including an aging model and an arcing model connected in parallel, was developed based on the physical behavior of aging insulation and the arcing phenomena occurring when the insulation was severely damaged. The characteristics of the incipient faults from the simulation were

compared with those from some experimental incipient fault cases. The comparison showed the experimentally obtained characteristics of terminal behaviors of the faulted transformer were similar to the simulation results from the incipient fault models. The Finite Element Method may be the most accurate approach for this purpose but it requires the knowledge of detailed design information that in most cases is not readily available.

Professor Joe Law [7] and his students built a transformer testing station, experimented on it, and accumulated a lot of useful information on transformer internal faults.

Since giant transformers in the US are almost always of single-phase built, the system that this thesis focuses on is that of a two-winding, shell-type, single-phase transformer with inter-turn fault occurred on the inner winding. The thesis derives a topology-based transformer inter-turn fault model with load and core saturation considered. Based on basic electric circuit theory, the thesis also derives equations for direct solution of the transformer inter-turn fault, which may find its important usage for transformer relay protection. The thesis discusses using PSPICE for the solution of transformer inter-turn fault as well.

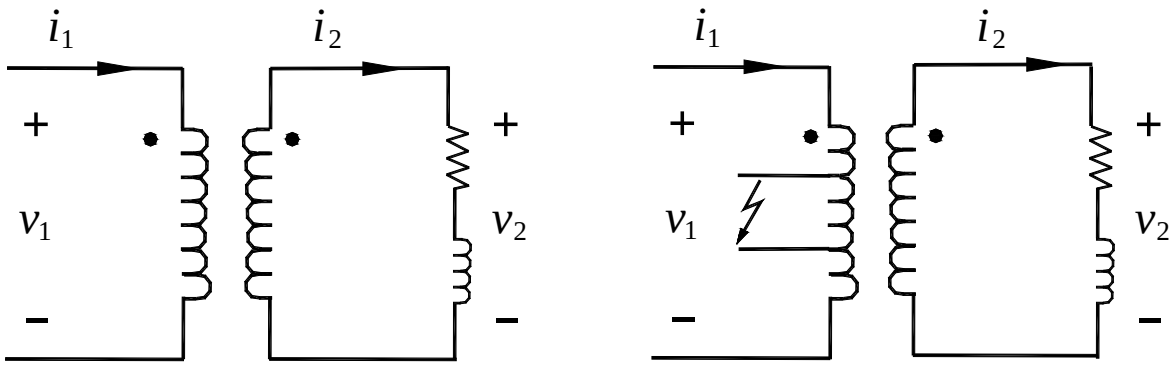

(a) Two-winding transformer. (b) Winding 1 has an inter-turn fault.

Fig. 1 Two winding, single-phase transformer with an inter-turn fault.

CHAPTER 2: TWO-WINDING, SHELL TYPE, SINGLE-PHASE TRANSFORMER AND ITS DUALITY-DERIVED EQUIVALENT ELECTRIC CIRCUIT

Chapter 2 introduces the principle of duality between an electric and a magnetic circuit. The equivalent electric circuit of a two-winding, shell-type, single-phase transformer mode is derived.

Duality is a powerful method for deriving an equivalent electric circuit from a magnetic circuit. This section concisely outlines the method following G. R. Slemon and Xusheng Chen [8, 9, 10, 11]. Since the method is not well-known to power system engineers, a concise outline of the method is given below.

Fig. 2 shows the cross section of a two-winding, shell-type, single-phase transformer. The flux pattern occurs when the magnetomotive force f_1 of the inner winding 1 is slightly greater than the magnetomotive force f_2 of the outer winding 2. Magnetic flux ϕ_1 takes the path of the center leg and the inner parts of the top and bottom yokes. A part of ϕ_1, ϕ_l, takes the path between the windings. The remainder, ϕ_2, takes the paths of the outer yokes and legs.

Fig. 3 shows the equivalent magnetic circuit of the transformer. Reluctances $\mathscr{R}_1$ and $\mathscr{R}_2$ present the paths taken by ϕ_1 and ϕ_2, respectively. The windings are represented by magnetomotive force (mmf) sources of $f_1 = N_1 i_1$ and $f_2 = N_2 i_2$. Reluctances $\mathscr{R}_1$ and $\mathscr{R}_2$ are in general nonlinear, but are often treated as linear around a steady-state operating point. In drawing Fig. 3, the transformer and its windings are assumed to have horizontal and vertical symmetry.

To derive the dual electric circuit from the magnetic circuit, a letter is marked in each mesh and one outside of the mesh as is shown in Fig. 4. Then the letters (A, B, and Z in this case) are linked through each circuit element, and rearranged to obtain Fig. 5.

It should be pointed out the R in an electric circuit stands for resistance and $\mathscr{R}$ in a magnetic circuit stands for reluctance.

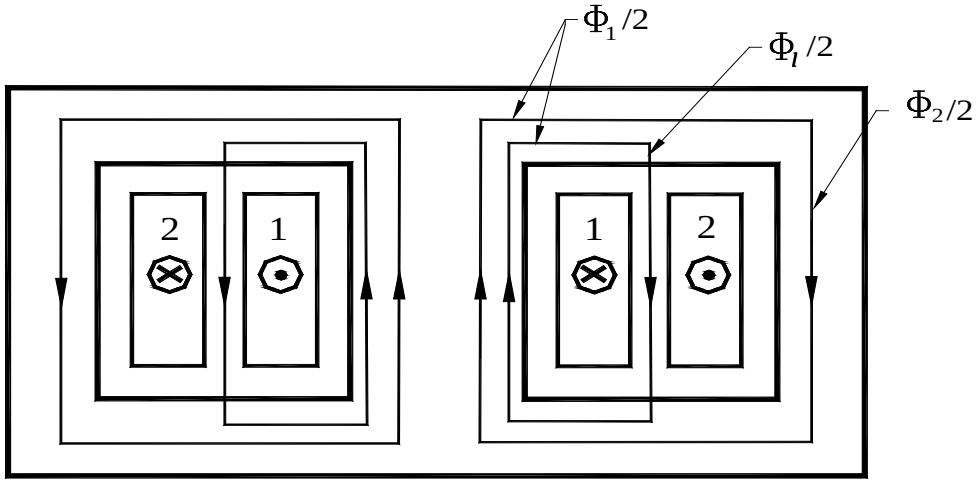

Fig. 2 The cross section of a two-winding, shell-type, single-phase transformer.

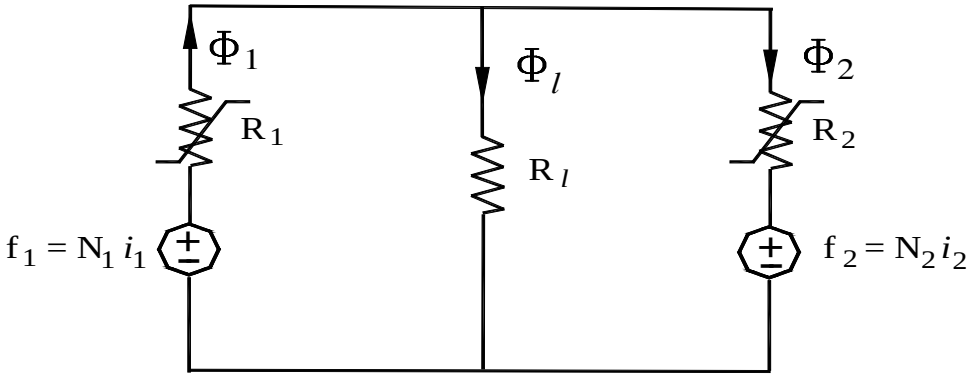

Fig. 3 Magnetic Circuit.

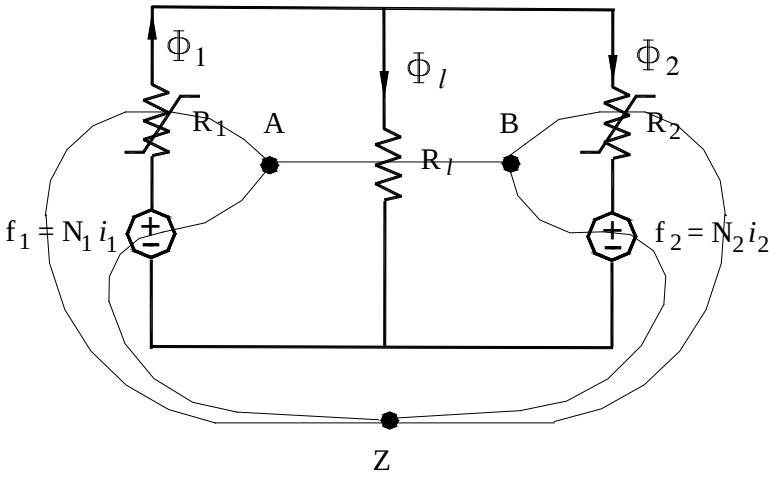

Fig. 4 The duality method applied to Fig. 3.

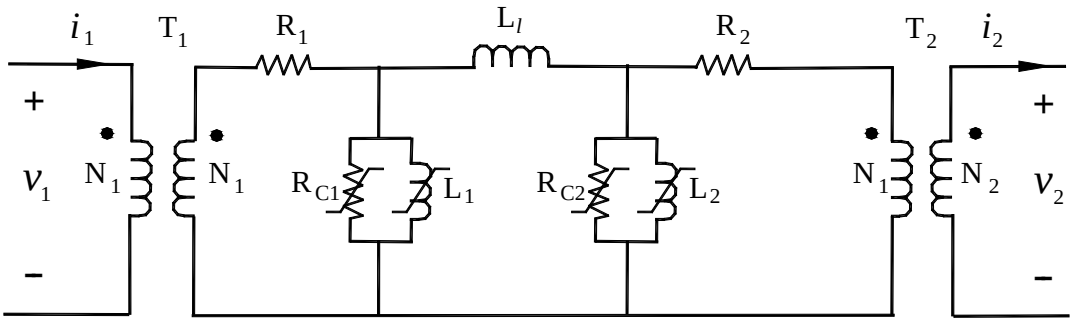

Fig. 5 Equivalent electric circuit of the two-winding, shell-type, single-phase transformer

Since Fig. 3 is somewhat difficult to visualize from Fig. 2; a simple explanation is given in Figs. 6 and 7.

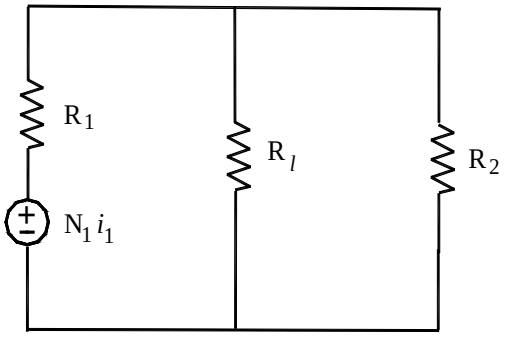

Fig. 6 Magnetic circuit when $\text{mmf}_1 = N_1 i_1$ is applied.

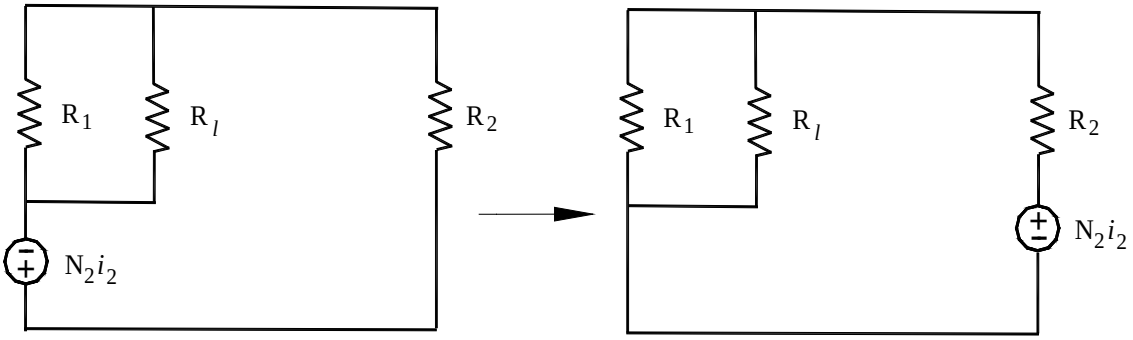

Fig. 7 Magnetic circuit when $\text{mmf}_2 = N_2 i_2$ is applied.

Fig. 6 is the magnetic circuit when winding 1 is excited and winding 2 is not excited (refer to Fig. 2). Fig. 7 is the magnetic circuit when winding 2 is excited and winding 1 is not excited. Note the polarity of magnetomotive force of winding 2, $N_2\ i_2$, is reversed. The reason for this is that Lenz's law requires that positive current i_2 generates a flux which is against its original flux (generated by i_1). When both windings are excited, Fig.3 results.

Comparing Figs. 4 and 5, one can see that the reluctances $\mathscr{R}_1$, $\mathscr{R}_2$, and $\mathscr{R}_l$ are changed to inductances L_1, L_2, and L_l; magnetomotive forces $f_1 = N_1\ i_1$ and $f_2 = N_2\ i_2$ are changed to voltage sources v_1 and v_2, respectively, and their related ideal transformers. Also added in the electric circuit are the winding resistances R_1 and R_2, and the core loss resistance R_{c1} and R_{c2}. Inductances L_1 and L_2, and core loss resistances R_{c1} and R_{c2}, are in general nonlinear. T_1 and T_2 are ideal transformers representing the turns ratio.

Remembering the analogy between an electric circuit and a magnetic circuit, voltage--magnetomotive force, current--flux, and resistance—reluctance, a straightforward derivation of those relationships, *in the linear case*, is given below.

$$f = R\,\phi = \phi / P \qquad \text{At} \tag{1}$$

$$f = N\,i \qquad \text{At} \tag{2}$$

$$v = \frac{d\lambda}{dt} = N\frac{d\phi}{dt} \qquad \text{V} \tag{3}$$

Substituting Eqs. (1) and (2) into Eq. (3) result in:

$$v = N\frac{d\phi}{dt} = N\frac{d(fP)}{dt} = N\frac{d(NiP)}{dt} = N^2P\frac{di}{dt} = L\frac{di}{dt} \qquad \text{V} \tag{4}$$

where $P = 1/R$ is the peameance and

$$L = N^2P \qquad \text{H} \tag{5}$$

CHAPTER 3: MAGNETIC AND ELECTRIC EQUIVALENT CIRCUITS OF THE TWO-WINDING, SHELL-TYPE, SINGLE-PHASE TRANSFORMER WITH AN INTER-TURN FAULT

In Chapter 3, duality is used to derive the equivalent electric circuit of the two-winding, shell-type, single-phase transformer when an inter-turn fault occurs on one of its windings and then the model is validated.

When an inter-turn fault occurs on winding 1 of the two-winding, shell-type, single-phase transformer as shown in Fig. 8, its simplified magnetic circuit is shown in Fig. 9. It should be pointed out that the representation of the leakage inductances is simplified to reveal the essence of the phenomenon. Even a little more detailed representation of the leakage inductances will destroy the symmetry of the transformer model and make the equivalent electrical circuit very complicated. Since the objective of this thesis is to develop a transformer model that can model inter-turn faults to reveal its characteristics, and since the equivalent resistance and inductance of the inter-turn fault changes in a large range and are unpredictable, the simplification of the circuit makes sense.

In Fig. 9 (page 12), The magnetomotive forces of winding 1 segment are:

$$f_{1A} = N_{1A}\, i_{1A}$$

$$f_{1B} = N_{1B}\, i_{1B}$$

$$f_{1C} = N_{1C}\, i_{1C}$$

$$N_{1A} = K_1\, N_1$$

$$N_{1B} = K_2\, N_1$$

$$N_{1C} = K_3\, N_1$$

$$K_1 + K_2 + K_3 = 1$$

$$N_{1A} + N_{1B} + N_{1C} = (K_1 + K_2 + K_3)\, N_1 = N_1$$

The leakage reluctances of winding 1 segment are assumed to be roughly proportional to the leakage inductance between the primary (winding 1) and secondary (winding 2) windings:

$R_{lA} = K_{1A}\ R_l$

$R_{lB} = K_{1B}\ R_l$

$R_{lC} = K_{1C}\ R_l$

$K_{1A} + K_{1B} + K_{1C} = K \leq 1$

It should be noted that we are studying a single-phase transformer, therefore, *A*, *B*, and *C* do not mean phases *A, B,* and *C*.

Applying duality to Fig. 10 and adding winding resistances R_{1A}, R_{1B}, and $R_{1C,}$ and core loss resistances R_{C1} and R_{C2}, results in Fig. 11A, the equivalent electric circuit of the two-winding, shell-type, single-phase transformer with inter-turn faults. R_2 is winding 2 resistance referred to winding 1. T_{1A}, T_{1B}, T_{1C}, and T_2 are ideal transformers. It is assumed that an ideal transformer only changes the voltage and currents according to the turns ratio and does not block the DC currents.

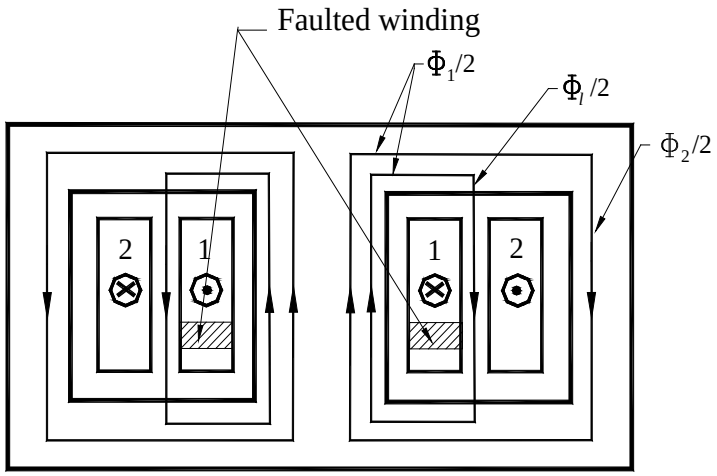

Fig. 8 The cross section of a two-winding, shell-type, single-phase transformer with an inter-turn fault.

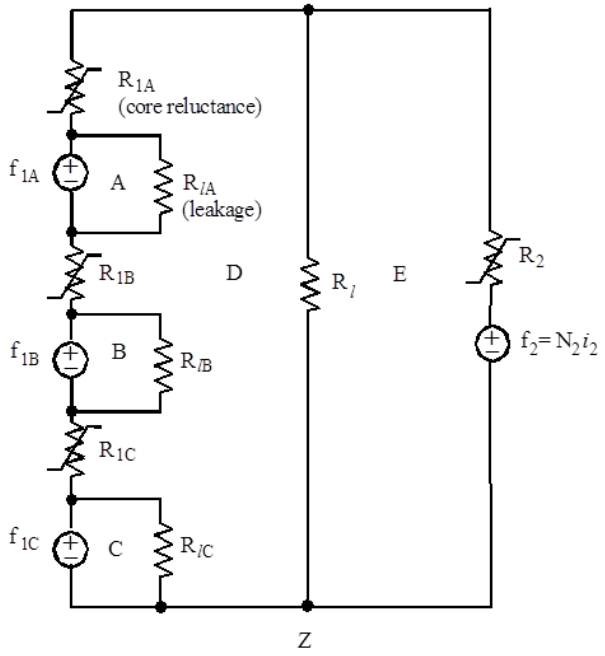

Fig. 9 Magnetic circuit of the transformer with an inter-turn fault.

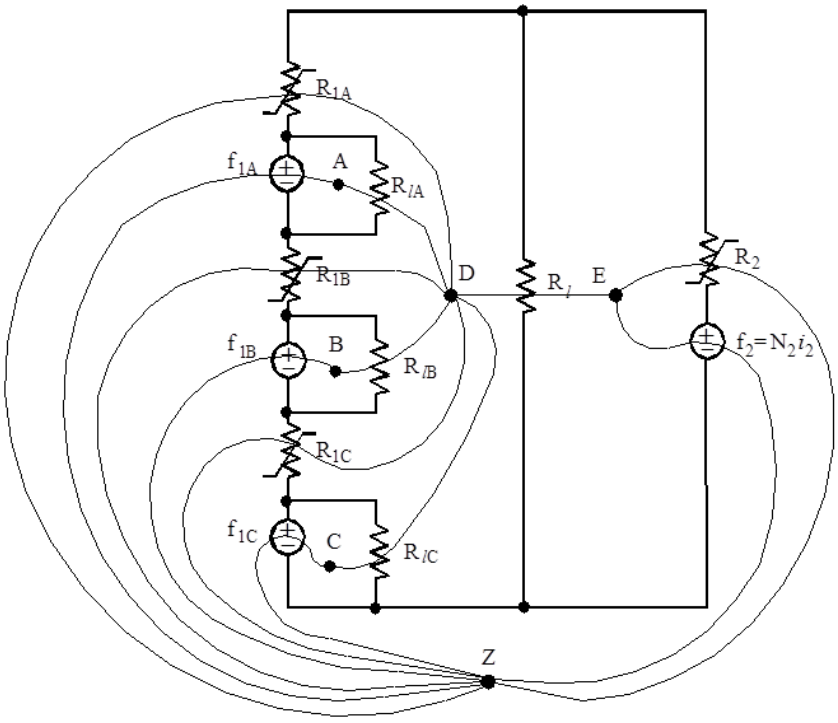

Fig. 10 Duality method applied on Fig. 9.

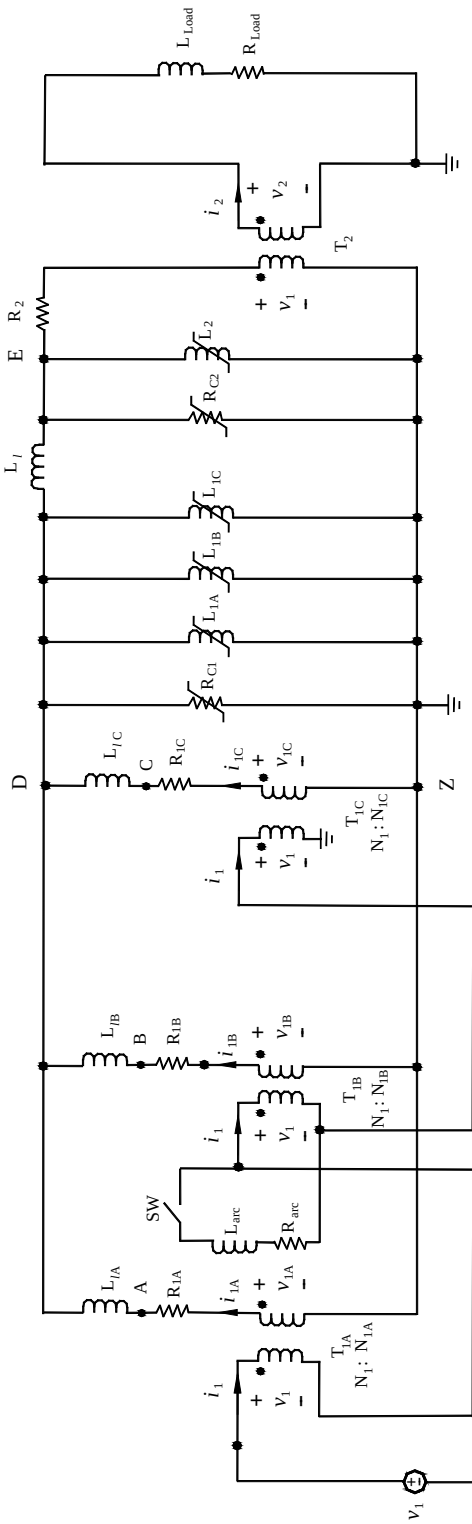

Fig. 11A The original duality-drived electric circuit of the two winding, shell-type, single-phase transformer with an inter-turn fault.

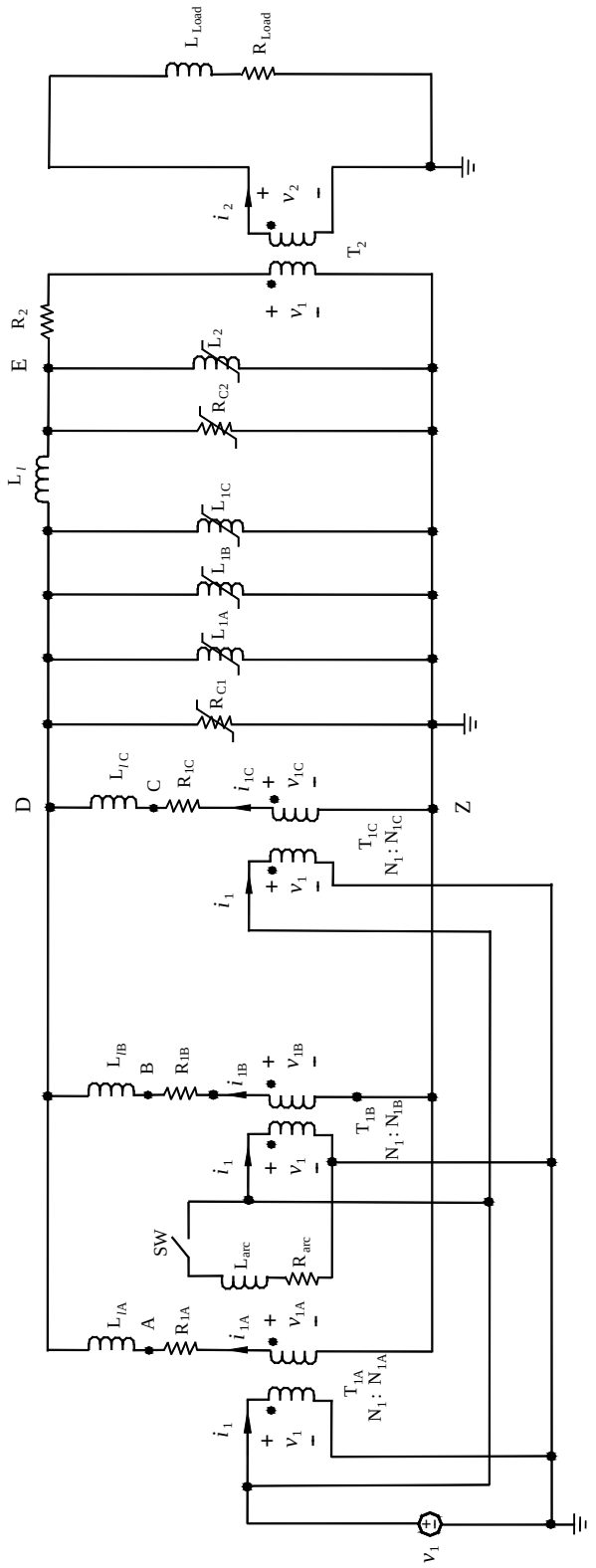

Fig. 11B The equivalent duality-drived electric circuit of the two winding, shell-type, single-phase transformer with an inter-turn fault.

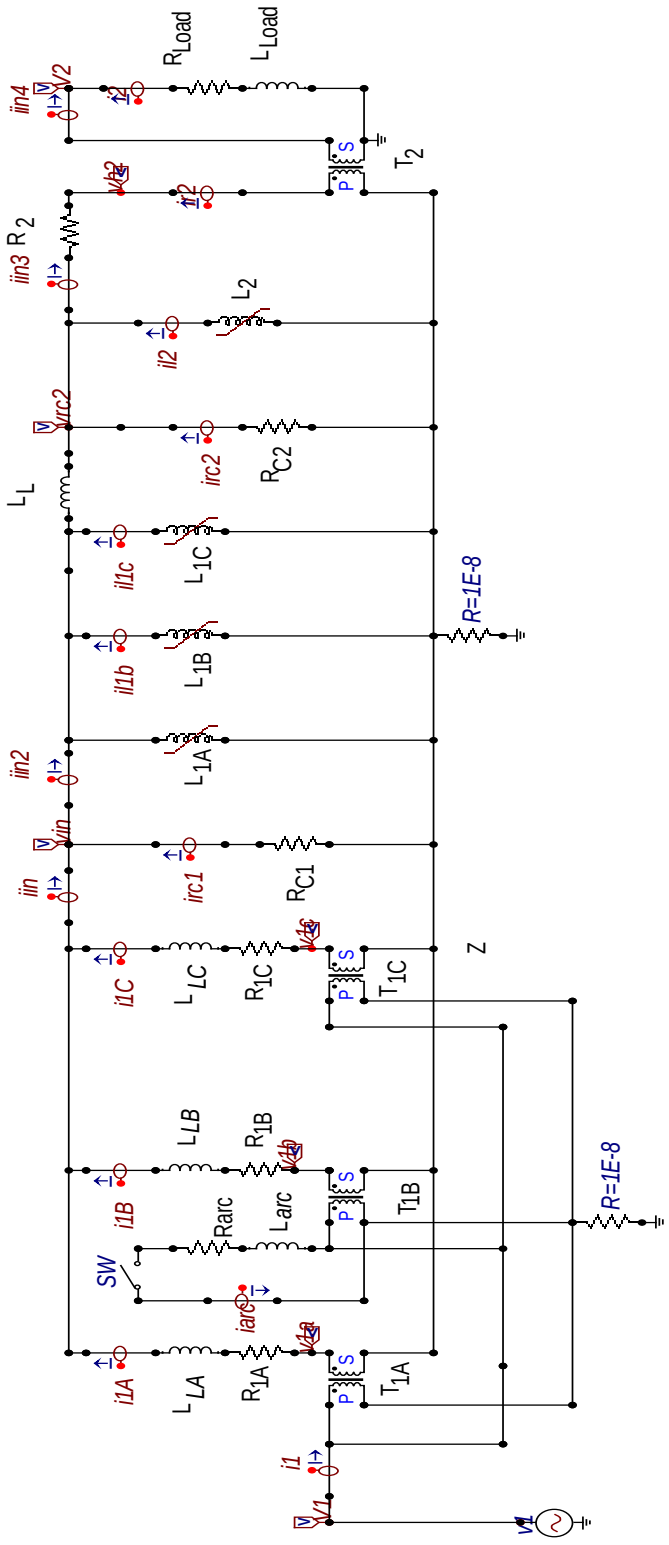

Fig. 11C The duality-derived ATP/EMTP circuit for single-phase transformer inter-turn fault

In Fig. 11A, T_{1A}, T_{1B}, T_{1C}, and T_2 are ideal transformers and R_{Load} and L_{Load} are an equivalent load resistance and inductance connected to transformer secondary.

In this Chapter, a time-controlled switch *SW* and a linear resistor R_{arc} in series with a linear inductor L_{arc} are used to model the transformer inter-turn fault. However, the developed transformer model can be easily adapted to much more complicated arc models such as the one proposed by Oliveira [3]: two parallel branches of insulated-gate bipolar transistors (IGBT) in series with a power diode. Transformer aging can be modeled by a capacitor in parallel with a resistor [4].

3.1 DEVELOPMENT OF THE TWO-WINDING, SHELL-TYPE, SINGLE-PHASE DUALITY-DERIVED TRANSFORMER MODEL

Initially Fig. 11A was used to model the transformer inter-turn fault occurred on the source side, but the model failed. Fig.11A gave completely unreasonable results. The reason is that ATP/EMTP software does not accept three Saturable Transformer Components connected in series. Fig. 11B is then used to model the transformer. The three Saturable Transformers Components are connected in parallel. Fig. 11B distributes the voltages among the segments of the inter-turn faulted winding according to the turns distribution. While it gives correct results for open-circuit and short-circuit tests, as well as full load test. It doesn't work for inter-turn faults; since the segment voltages are fixed, it doesn't represent the inter-turn fault correctly. It is concluded that ATP/EMTP cannot model the duality-derived transformer inter-turn fault that occurred at the source side. In order to simulate transformer inter-turn faults, the source and the load side of Fig. 11B is swapped (see Fig. 20), and the inter-turn fault occurs at load side, the revised model (Fig. 20) works reasonably although not accurately.

The derivation of the topology-based and duality-derived transformer model is now complete.

3.2 VERIFICATION OF THE DUALITY MODEL

Mork's 5-legged stacked core transformer, 12470GRY/7200 : 208/120 was used to verify the duality-derived transformer inter-turn fault model [13]. The transformer is adjusted to a single-phase transformer with the following data:

$S_r = 150 / 3 = 50$ kVA $\quad V_{rH} / V_{rL} = 7200 / 120 = 60$ V/V

$X_{HL} = 31.586$ Ω $\quad L_{HL} = X_{HL} / (2\pi 60) = 83.784$ mH

$I_{rH} = S_r / V_{rH} = 6.944$ A $\quad I_{rL} = S_r / V_{rL} = 416.67$ A

$Z_{rH} = V_{rH} / I_{rH} = 1036.87$ Ω $\quad Z_{rL} = V_{rL} / I_{rL} = 0.288$ Ω

$\Lambda_{rH} = V_{rH} / (2\pi f) = 7200 / (2\pi f) = 19.099$ Wbt

$\Lambda_{rL} = V_{rL} / (2\pi f) = 120 / (2\pi f) = 0.3183$ Wbt

Where

S_r -- kVA rating of the transformer

X_{HL} -- leakage reactance at 60 Hz

L_{HL} -- leakage inductance

I_{rH} , I_{rL} -- HV and LV side rated currents

Z_{rH}, Z_{rL} -- HV and LV side rated impedances

The λ-i curve given by Mork [13] is used to compute the λ-i curves for nonlinear inductances L_2, L_{1A}, L_{1B}, and L_{1C}, which are shown in Tables 3.1 and 3.2.

Table 3.1 is for 33% inter-turn fault and Table 3.2 is for 8% inter-turn fault (the distribution of the segments are 46%, 8%, and 46%).

Table 3.1 33% TRANSFORMER INTER-TURN FAULT ATP MODEL DATA TABLE (Voltage *v* in V, current *i* in A, resistance R in Ω, and inductance L in mH)

Single Phase Transformer		**7200 : 120V**	**50 KVA**	
v_1 = 10182(peak)		$R_{C1} = 10^5$		L_L = 83. 8
R_{Load} = 0.2304		$R_{C2} = 10^5$		L_{LA} = 5.586
L_{Load} = 0. 4584		R_1 = 3. 9203		L_{LB} = 5.586
R_{1A} = 1.3067		R_2 = 0.0012		L_{LC} = 5.586
R_{1B} = 1.3067		R_{arc} = 9.54		L_2 = 81.12
R_{1C} = 1.3067		L_{arc} = 18.98		K= 0. 4
				[L_{LA} =(83. 8)/6*0.4]
N1A:N1	N1B:N1	N1C:N1	N1:N2 =	
2400:7200	2400:7200	2400:7200	7200:120	
	For L2	For L1A	For L1B	For L1C
λ1 (Wbt)	iL2 (A)	i1A (A)	i1B (A)	i1C (A)
4.524	0.01060833	0.0035361	0.0035361	0.0035361
9.096	0.01083333	0.0036111	0.0036111	0.0036111
11.364	0.01624167	0.0054139	0.0054139	0.0054139
13.53	0.02518333	0.0083944	0.0083944	0.0083944
14.7	0.03005833	0.0100194	0.0100194	0.0100194
15.756	0.03893333	0.0129778	0.0129778	0.0129778
16.878	0.045375	0.015125	0.015125	0.015125
18.054	0.06161667	0.0205389	0.0205389	0.0205389
19.152	0.08731667	0.0291056	0.0291056	0.0291056
20.304	0.12333333	0.0411111	0.0411111	0.0411111
21.45	0.16728333	0.0557611	0.0557611	0.0557611
22.506	0.21411667	0.0713722	0.0713722	0.0713722
24.804	0.35266667	0.1175556	0.1175556	0.1175556
27.012	0.70248333	0.2341611	0.2341611	0.2341611

Table 3.2 8% TRANSFORER INTER-TURN FAULT ATP MODEL DATA TABLE (Voltage *v* in V, current *i* in A, resistance R in Ω, and inductance L in mH)

Single Phase Transformer		**7200 : 120V**	**50 KVA**	
v_1 = 169(peak)	R_{Load3} = 382	$R_{C1} = 10^5$	L_2=81.12	
R_{Load1} = 382	L_{Load3} = 757	$R_{C2} = 10^5$	L_L = 83.8	
L_{Load1} = 757	R_{1A} = 1.803	R_2= 4.32 (refer to R_1 side)	L_{LA} = 7.71	
R_{Load2} = 66.4	R_{1B} = 0 .314	R_{arc} = 3	L_{LB} = 1.34	
L_{Load2} = 132	R_{1C} = 1.803	L_{arc} = 4.5	L_{LC} = 7.71	
$N_{1A}:N_1$	$N_{1B}:N_1$	$N_{1C}:N_1$	$N_1:N_2$ =	
3312:7200	576:7200	3312:7200	7200:120	
	For L_2	For L_{1A}	For L_{1B}	For L_{1C}
λ_1 (Wet)	i_{L2} (A)	i_{1A} (A)	i_{1B} (A)	i_{1C} (A)
4.524	0.01060833	0.00488	0.000849	0.0048798
9.096	0.01083333	0.004983	0.000867	0.0049833
11.364	0.01624167	0.007471	0.001299	0.0074712
13.53	0.02518333	0.011584	0.002015	0.0115843
14.7	0.03005833	0.013827	0.002405	0.0138268
15.756	0.03893333	0.017909	0.003115	0.0179093
16.878	0.045375	0.020873	0.00363	0.0208725
18.054	0.06161667	0.028344	0.004929	0.0283437
19.152	0.08731667	0.040166	0.006985	0.0401657
20.304	0.12333333	0.056733	0.009867	0.0567333
21.45	0.16728333	0.07695	0.013383	0.0769503
22.506	0.21411667	0.098494	0.017129	0.0984937
24.804	0.35266667	0.162227	0.028213	0.1622267
27.012	0.70248333	0.323142	0.056199	0.3231423

3.3 SIMULATION RESULTS

The following six case studies show the validity of the duality-derived model.

Test Case 1 Fig. 11B is used to simulate the full load condition without faults. The voltage applied to the HV side of the model is the rated voltage of 7200 V RMS, or the amplitude of 10182.34 V, and the voltage source initial angle is 0^o. The load impedance referred to LV side is: $Z_{L2} = R_{L2} + jX_{L2} = 0.2304 + j\,(2\pi 60)\,(0.4584 / 1000) = 0.2304 + j\,0.1728 = 0.288 \angle 36.87^o\ \Omega$

Fig. 12 and Fig. 13 show the input voltage and current waveforms. The RMS value of the current waveform is *6.944 A* referred to the HV side.

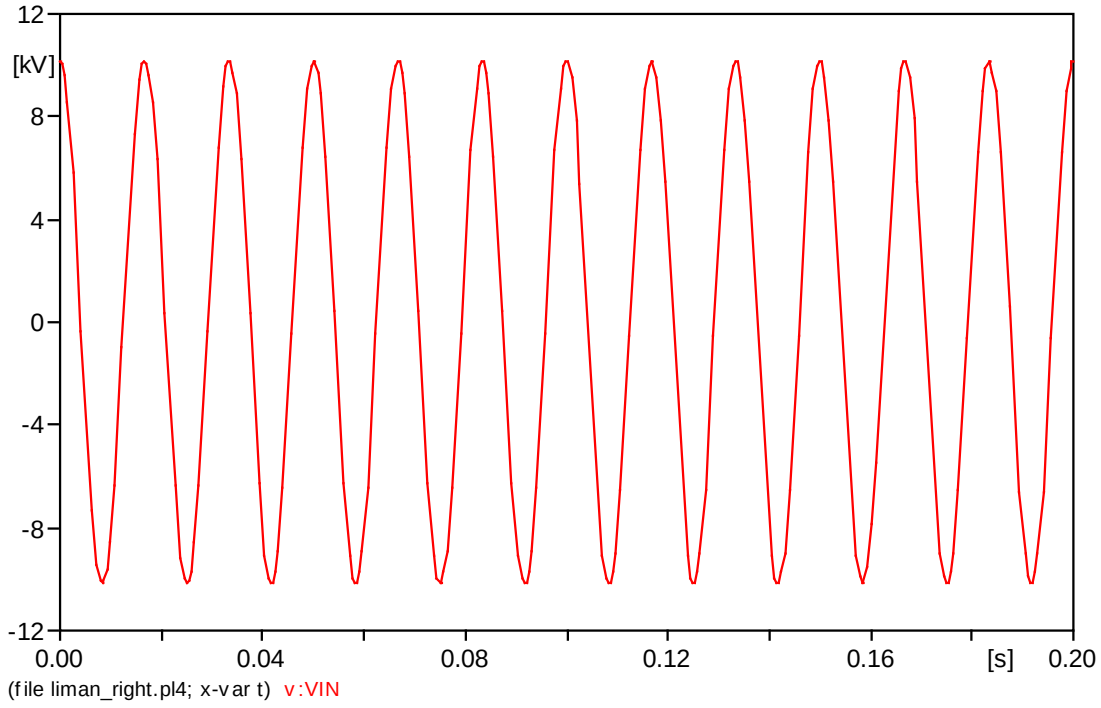

Fig. 12 Full Load Test Input Voltage v_{in} Waveform

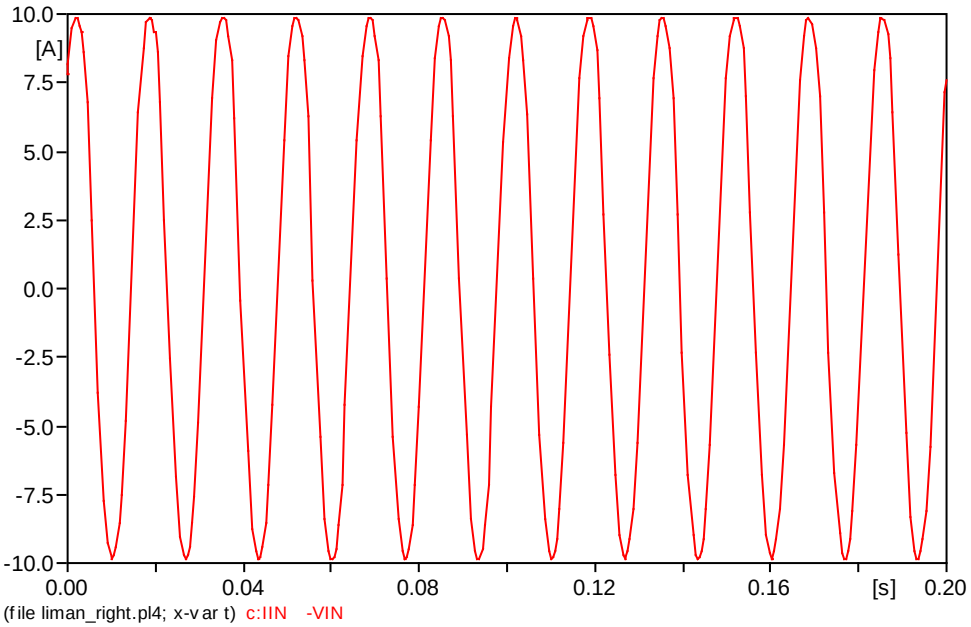

Fig. 13 Full Load Test Input Current i_{in} Waveform

Test Case 2 simulates transformer excitation from the primary with secondary open. Figs. 14 and 15 show the input voltage and current waveforms. The rms value of the excitation current or no load current is $I_o = 0.35\ A$, which is approximately *5%* of high voltage side rated current.

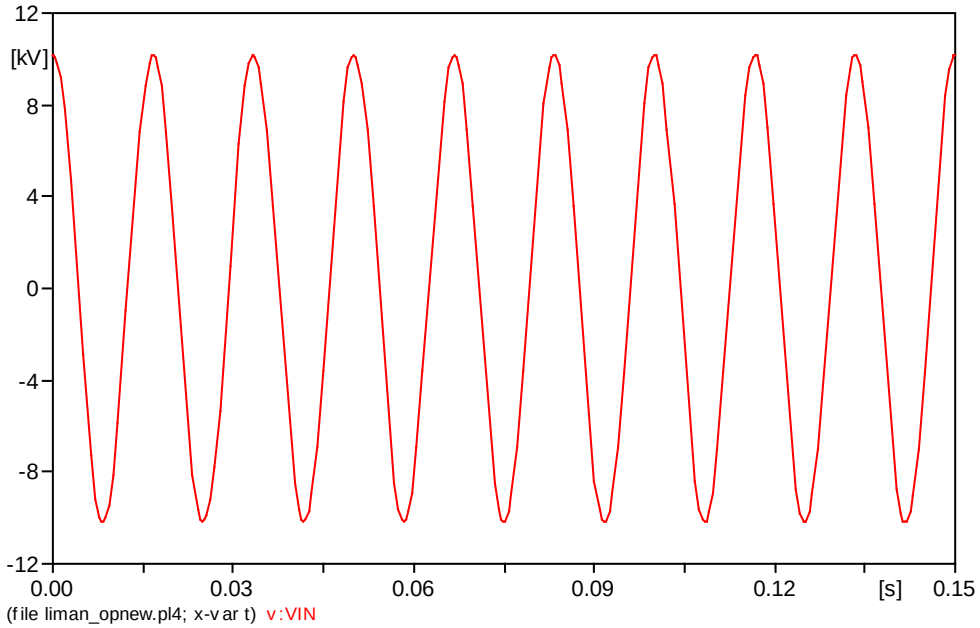

Fig. 14 Open Circuit Test Input Voltage v_{in} Waveform

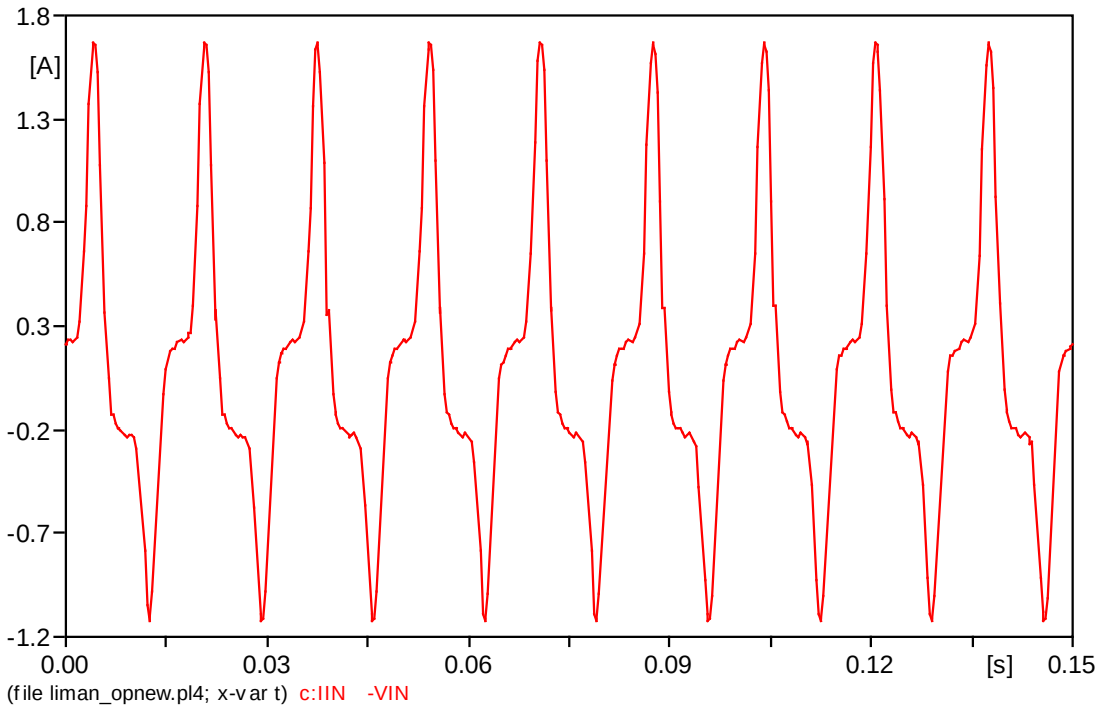

Fig. 15 Open Circuit Test Input Current i_{in} Waveform

Test Case 3 simulates the standard transformer short-circuit test. The voltage applied to the HV side of the model is rated voltage of 7200 V rms, or $v_1(t) = 10182.34 \cos (2 \pi 60 t + \alpha) = 10182.34 \cos (376.99 t + \alpha)$ V, the voltage angle is $\alpha = 0^o$, and I = 0.76 A rms. Figs. 16 and 17 show the waveforms of the applied HV voltage and the short circuit current. The short-circuit reactance $X_{HL} = 31.586\ \Omega$ is given by Mork [13]. Since the leakage inductances are added in the model, the leakage inductance L_l is reduced from *83.784 mH* to *81.12 mH*, such that the short circuit reactance of the model matches exactly as Mork's data [13].

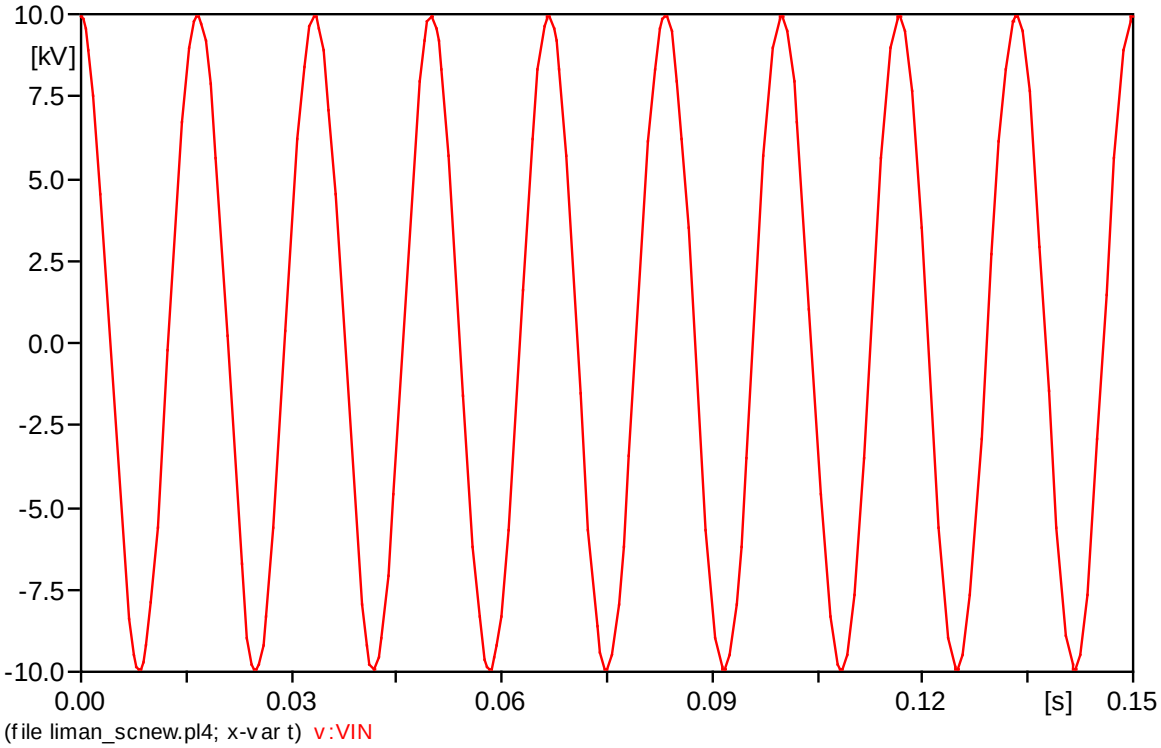

Fig. 16 Short Circuit Test Input Voltage v_{in} Waveform

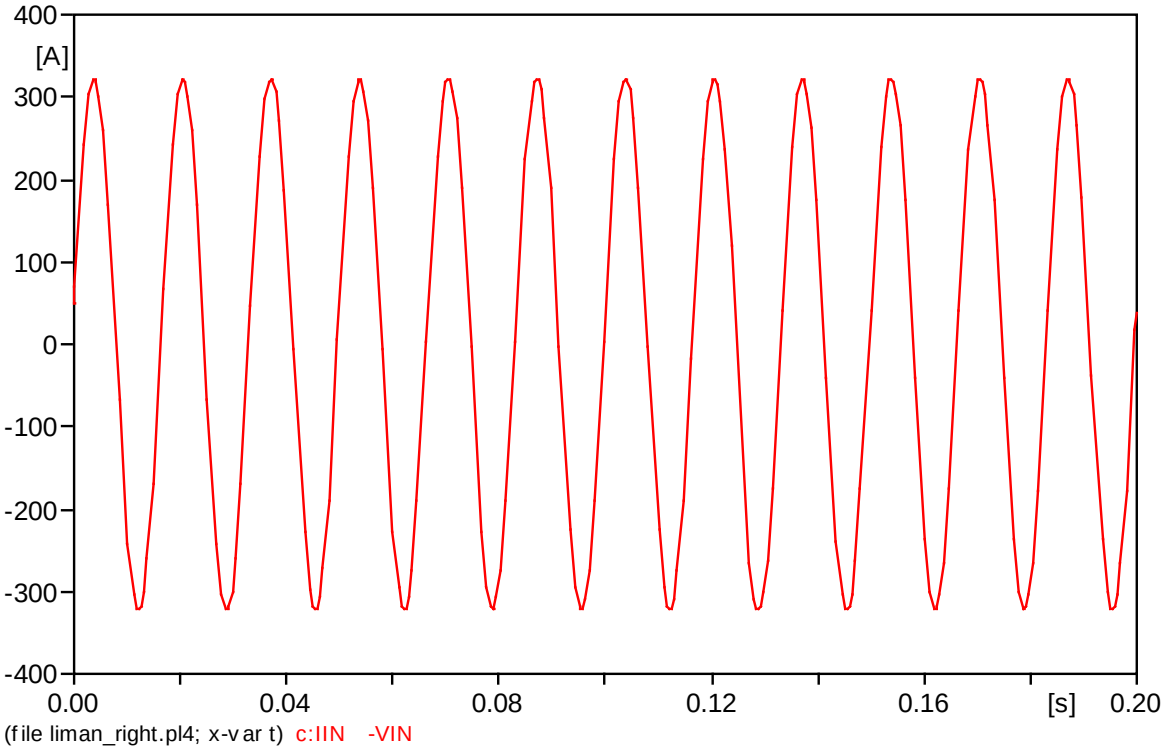

Fig. 17 Short Circuit Test Input Current i_{in} Waveform

Test Case 4 simulates the inrush current of the transformer. The first cycle peak value of the current is 9.88 A, which is completely offset and slightly larger than the rated HV peak current. The switching angle is -90°.

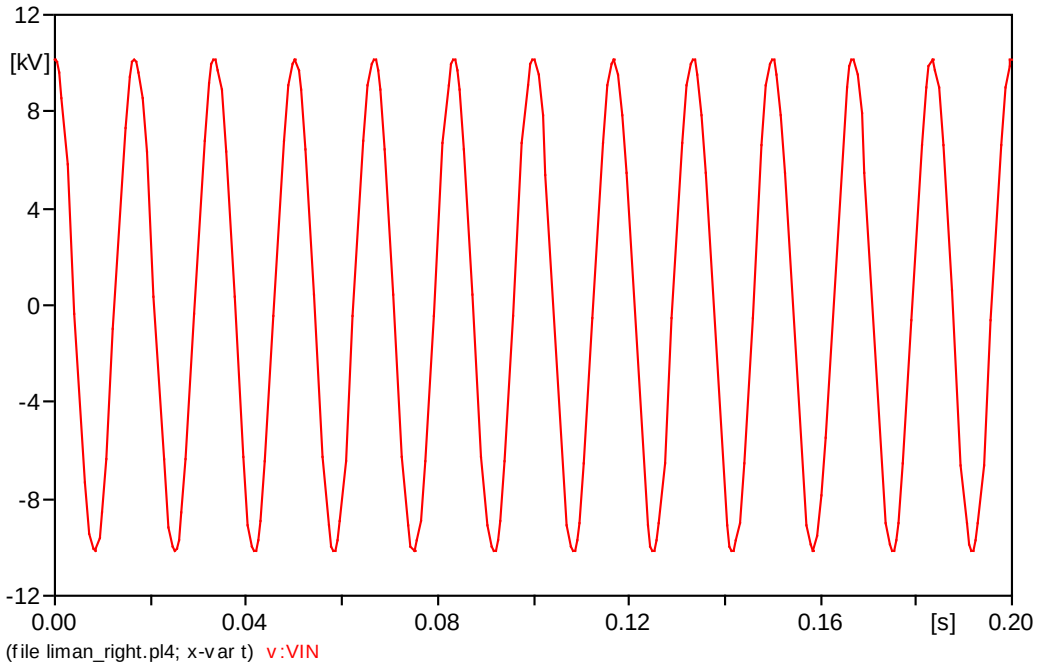

Fig. 18 Inrush Test Input Voltage v_{in} Waveform

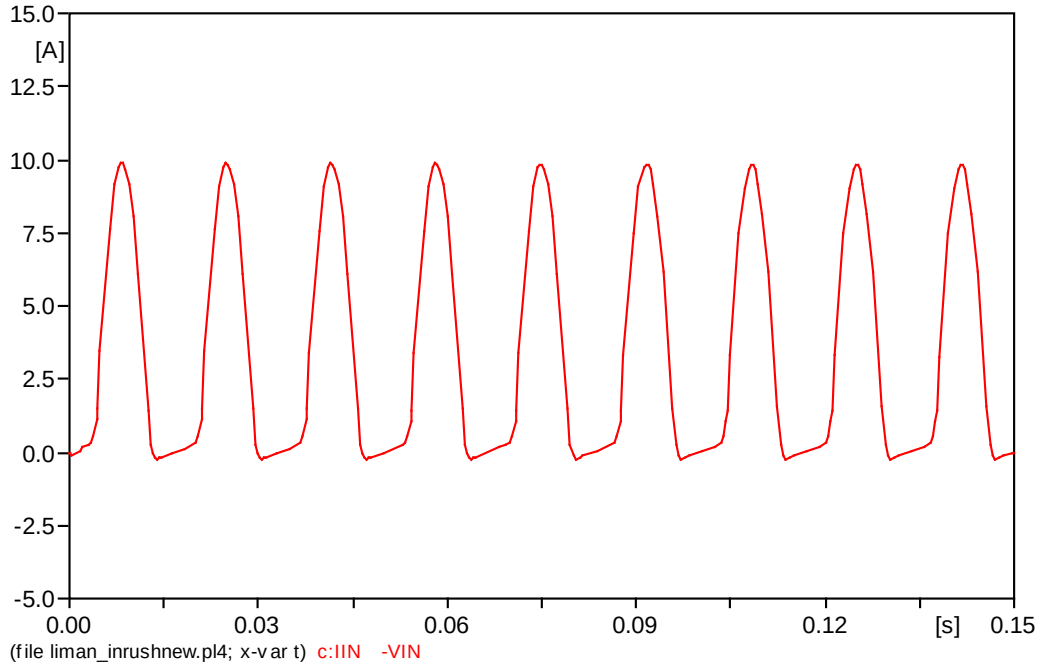

Fig. 19 Inrush Test Input Current i_{in} Waveform

Test Case 5 simulates the inter-turn fault for a 33% turn-to-turn fault and during a full load condition.

Since Fig.11B cannot model the duality-derived transformer inter-turn fault that occurred at the source side as mentioned previously, Fig. 11B is revised by swapping the source and load sides, the rated voltage 120 V rms or $v_2 = \sqrt{2} * 120 * \cos(\omega t + \alpha) = 169 \cos(2\pi 60 t + \alpha)$ was applied to the LV side the R_{load} of $(0.2304 + j0.1728) \times 3600 = 829.44 + j622.14$ Ω was connected to the former source side (see Fig. 20). Since Saturable Transformer Components of ATP/EMTP do not work for transformer series connection, the load for each segment of the faulted winding was distributed according to the turns of each segment: $R_{load1} = R_{load2} = R_{load3} = 276.5$ ohm, and $L_{load1} = L_{load2} = L_{load3} = 550$ mH (see Fig. 20). The arc resistance and inductance were set at 9.54 Ω and 18.98 mH, respectively. The simulation starts with $\alpha = 0^o$ and the switch is opened at the beginning and closed at 0.2 seconds, opened at 0.4 seconds, reclosed at 0.6 seconds.

When switch is closed, the peak current in the arc circuit is 223.5 A (Fig. 21), and the peak current i_2 in the supplying side (HV) is 83.5A (Fig. 23), which is 7.35 rated full load peak current. Since the terminal current for the inter-turn fault is inversely proportional to the turns ratio, the terminal current for 8% fault is four times smaller than that of the 33% fault (33% / 8% = 4.125).

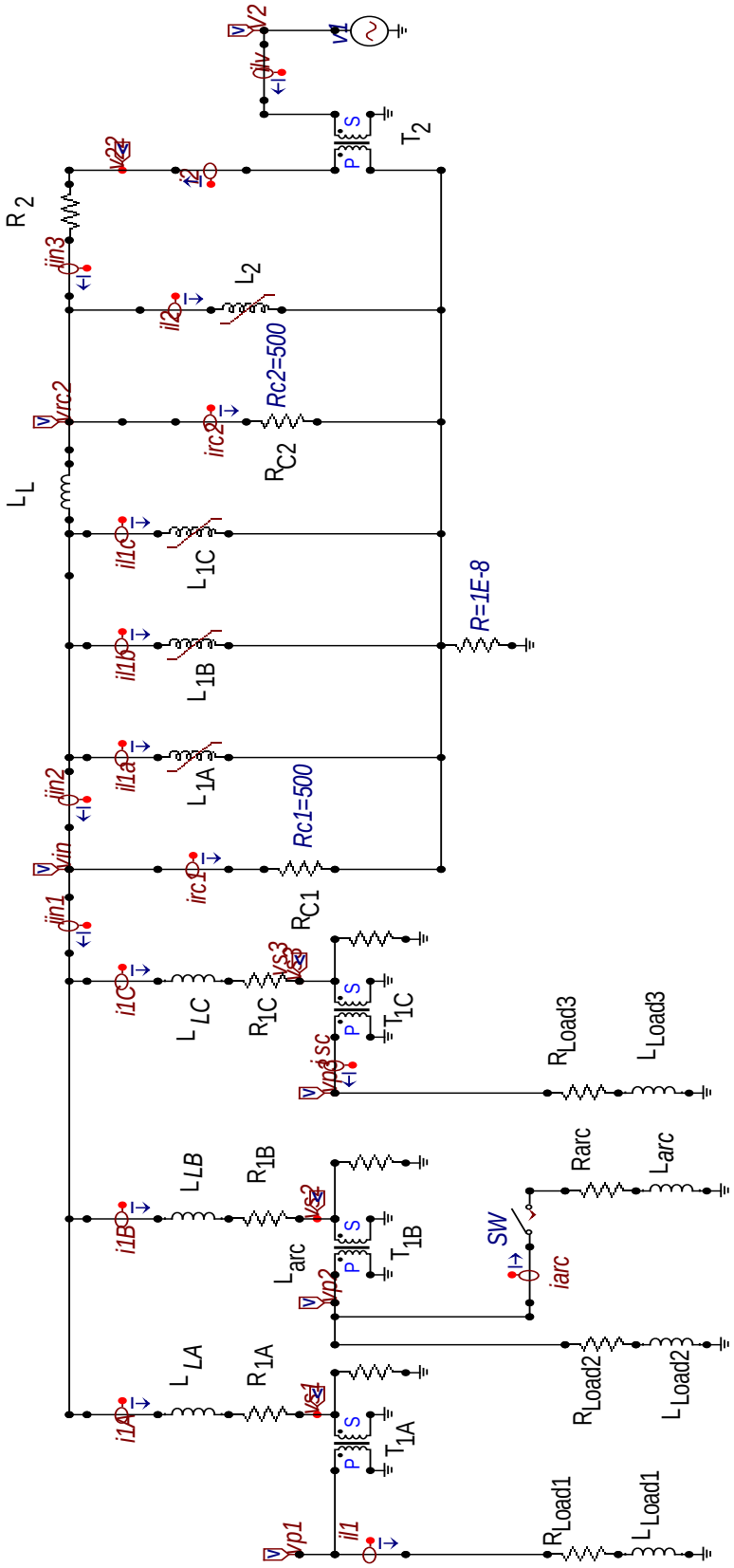

Fig. 20 The revised duality-derived ATP model for single-phase transformer inter-turn fault

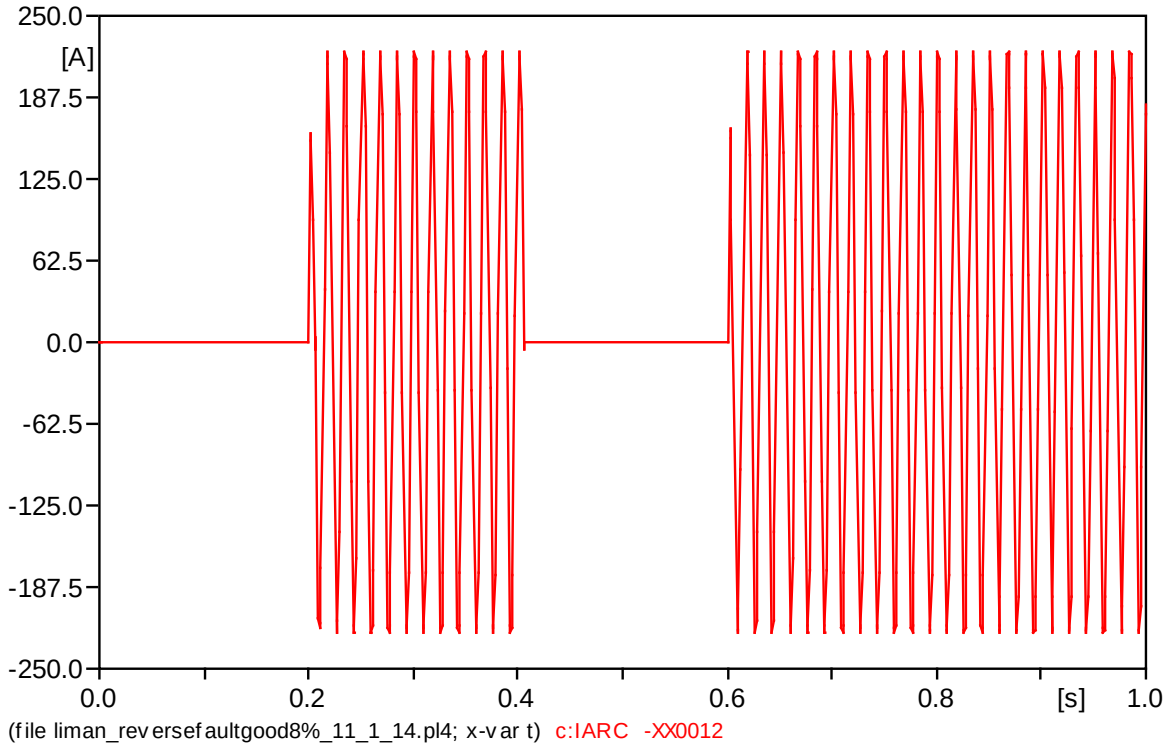

Fig. 21 33% Inter-Turn Fault Test Fault Current i_{arc} Waveform

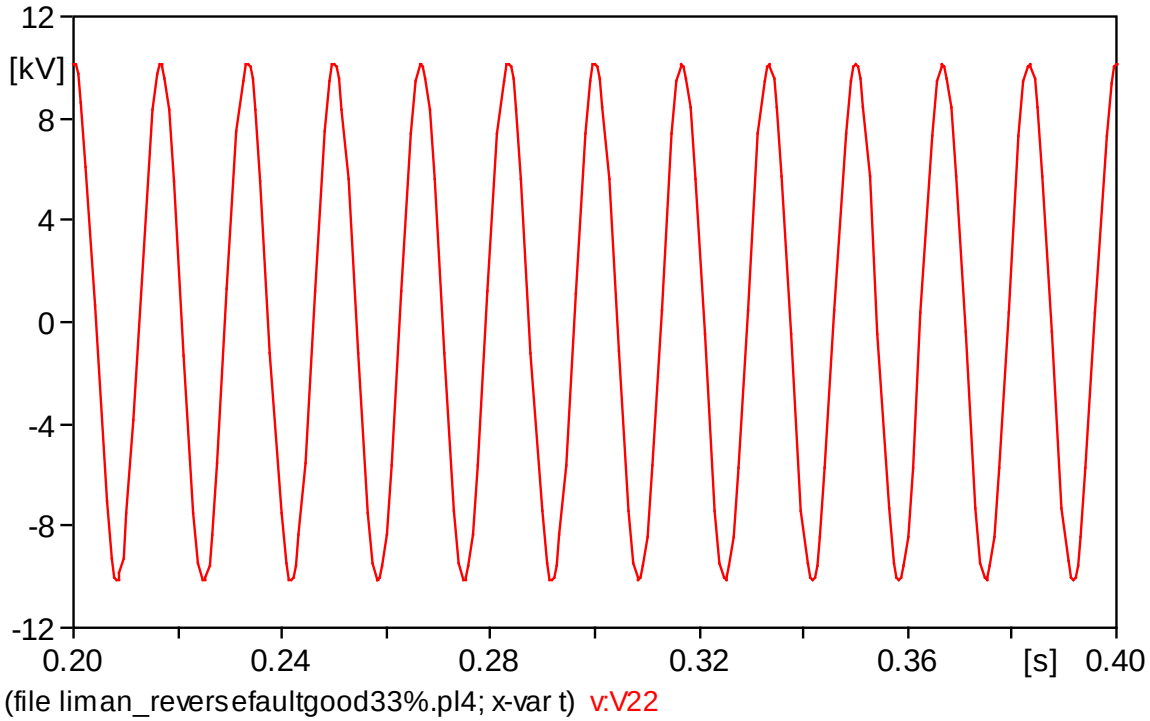

Fig. 22 33% Inter-Turn Fault Test Input Voltage v_{22} Waveform

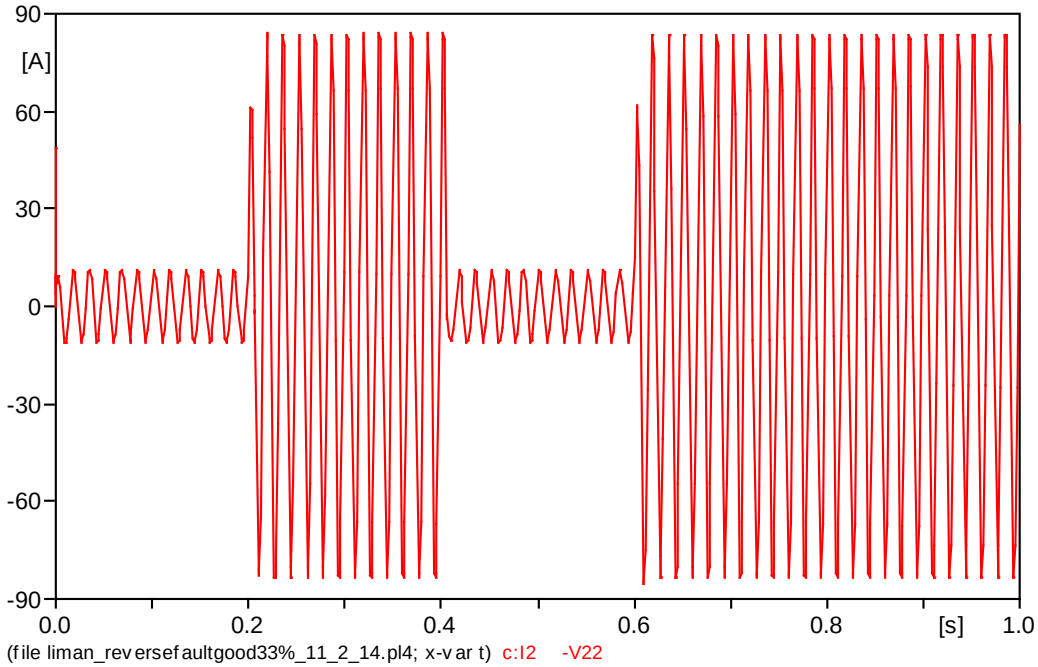

Fig. 23 33% Inter-Turn Fault Test Input Current i_2 Waveform

Test Case 6 simulates the inter-turn fault for an 8% turn-to-turn fault and with a full load.

The arc resistance and inductance are *3* Ω and *4.5 mH*, respectively. The simulation starts with voltage angle $\alpha = 0^o$ and the switch is opened at the beginning and closed at 0.2 seconds, opened at 0.4 seconds, reclosed at 0.6 seconds.

When switch is closed, the peak current in the arc circuit is 223.5 A, and the peak current in the HV supplying side is 28.4 A, which is 1.84 rated full load peak current.

Compare with 33% inter-turn fault, although the arc resistance and inductance are adjusted so that the arc current in the two cases are the same, the currents in the source side are substantially different. The smaller the faulted turns, the larger the current in the turns and the smaller the current in the terminals.

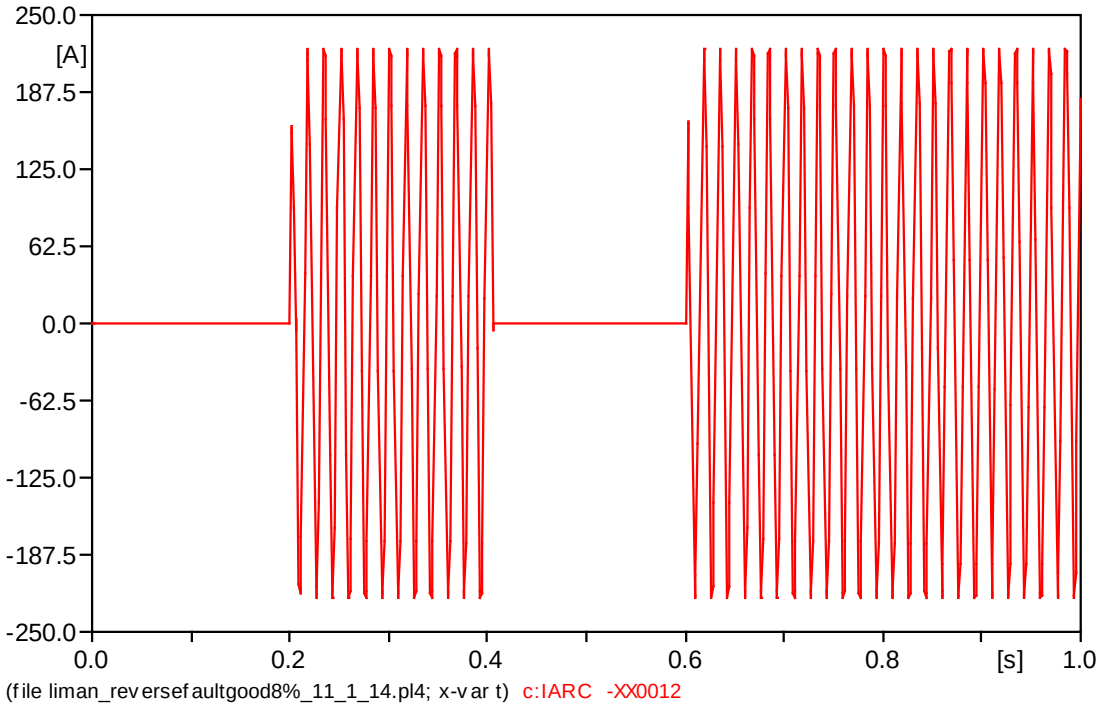

Fig. 24 8% Inter-Turn Fault Test Fault Current i_{arc} Waveform

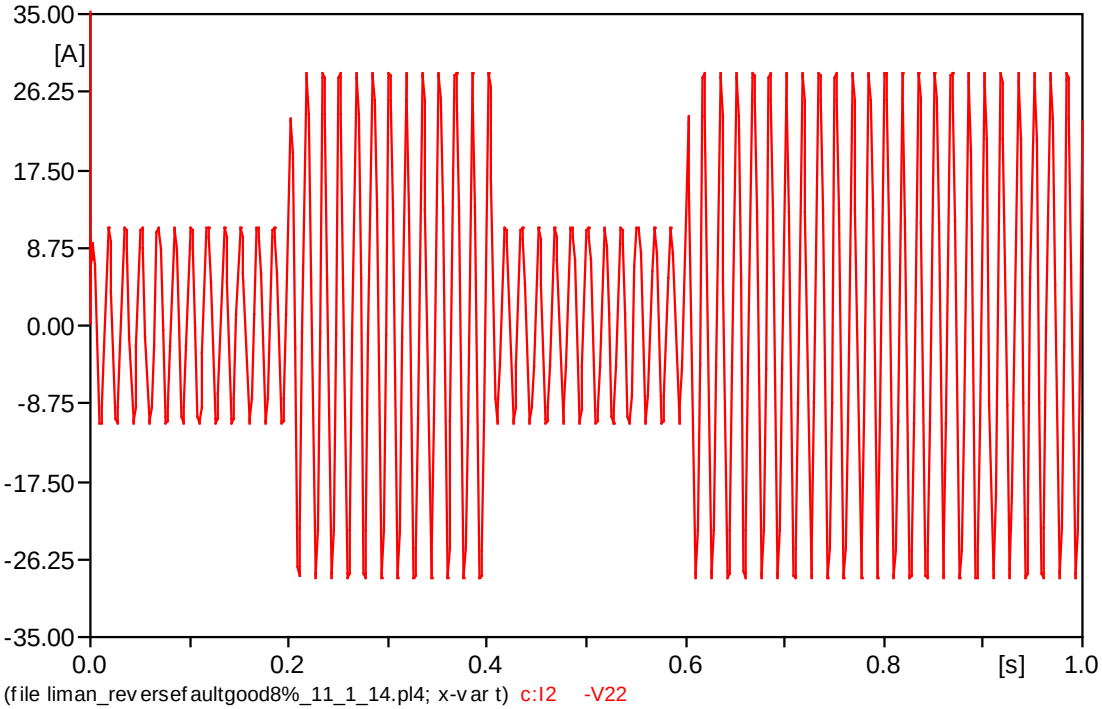

Fig. 25 8% Inter-Turn Fault Test Input Current i_2 Waveform

3.4 VERIFICATION OF THE DUALITY MODEL PERFORMED BY A 55KVA TRANSFORMER SHORT CIRCUIT LABORATORY TEST DATA.

Transformer short circuit laboratory test data provided by EE professor Dr. Brian Johnson of University of Idaho is used to test the revised single-phase transformer inter-turn fault duality model (Table 3.3). The transformer is shorted and opened (taps at 100%) at the transformer secondary; the transformer is shorted at 10% of the windings at transformer secondary as well (taps at 10%). The transformer was adjusted to a single-phase transformer with U of I laboratory test data; for clarity in revealing the essence of the inter-turn fault of the single-phase transformer, the tertiary of the transformer is not included in this thesis.

Transformer Data: 55kVA, 240/240V/24V, three-phase Delta/Y/Delta (HV, LV, and Tertiary). The transformer is adjusted to an 18.33kVA single-phase transformer. The single-phase transformer data is listed below (r means “rated):

$S_r = 18.33 \quad kVA$

$N_H = 50 \text{ turns}$

$N_L = 50 \text{ turns}$

$N_T = 5 \text{ turns}$

$V_{rH} = 240 \ V$

$V_{rL} = 240 \ V$

$V_{rT} = 25 \ V$

$I_{rH} = S_r / V_{rH} = 76.39 \ A$

$I_{rL} = S_r / V_{rL} = 76.39 \ A$

$Z_{rH} = V_{rH} / I_{rH} = 3.142 \ \Omega$

$Z_{rL} = V_{rL} / I_{rL} = 3.142 \ \Omega$

$L_{rH} = Z_{rH} / (2\pi f) = 8.334 \ mH$

$L_{rL} = Z_{rL} / (2\pi f) = 8.334 \ mH$

$\Lambda_{rH} = V_{rH} / (2\pi f) = 240 / (2\pi f) = 0.6366 \quad Wbt$

$\Lambda_{rL} = V_{rL} / (2\pi f) = 240 / (2\pi f) = 0.6366 \quad Wbt$

TABLE 3.3 55 KVA TRANSFORMER SHORT/OPEN CIRCUIT LABORATORY TEST DATA (Taps at 100% -- complete LV winding; taps at 10% -- 10% of the LV winding)

Winding Configuration				Taps @ 100%				Taps @ 10% X = (0.1)240 = 24	
Source	**Shorted/Open**	**Open**	**Phase**	**Vsc (V)**	**Isc (A)**	**Voc (V)**	**Ioc (A)**	**Vsc (V)**	**Isc (A)**
H	X	Y	A	7.9	107.7	241	12.11	14.6	11.85
H	X	Y	B	8.1	121.2	243	9.67	11.5	11.6
H	X	Y	C	7.3	112.7	237	8.14	13.4	15.2

V_{sc} and I_{sc} data were measured from source side. H: Primary (240V), X: Secondary (240V with taps), Y: Tertiary (25V). H is connected in Delta, X is connected in Wye, Y is connected in Delta. When V_{sc} and V_{oc} were measured from H and Y windings, they were measured as line-to-line voltages.

Below is the transformer short circuit test diagram based on Table 3.3.

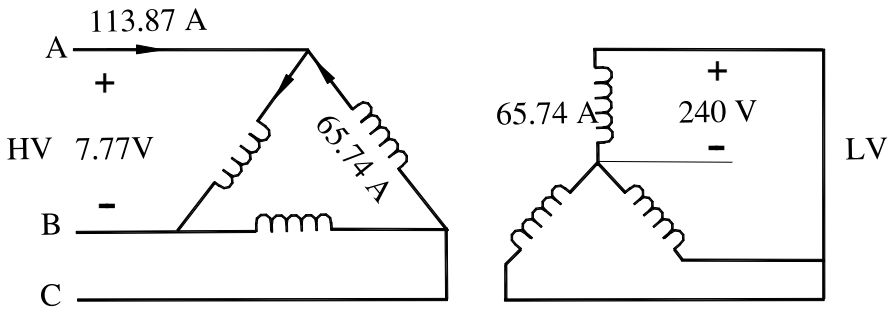

(a) Three-phase connetio short circuit diagram

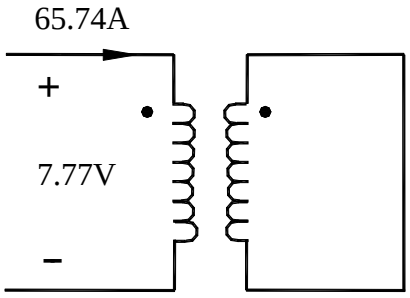

(b) Single-phase connection short circuit diagram

Fig. 26 Short circuit diagrams for the labratory testing transform

Based on transformer laboratory data, for taps at 100% short circuit test at the transformer secondary, we can average the three results, leading to:

$V_{SC} = (7.9 + 8.1 + 7.3) / 3 = 7.77\ V$

$I_{SC} = (107.7 + 121.2 + 112.7) / 3 = 113.87\ A$

$Z_{in\_3\phi} = [(7.77 / \sqrt{3})] / 113.87 = 0.0394\ \Omega$

$Z_{in\_1\phi} = 7.77\ V / 65.74\ A = 0.118\ \Omega$

$V_{OC} = (241 + 243 + 237) / 3 = 240.33\ V$

$I_{OC} = (12.11 + 9.67 + 8.14) / 3 = 9.97\ A$

Since the short circuit power is not given, so typical transformer data are used here, the ratio between the transformer resistance and reactance is 1 to 6 [14].

Thus the impedance angle of Z_{HL} *is* $\theta = 80^o$, which results in

$Z_{HL} = 0.118\ \underline{/80^o}\ \Omega$

$R_L = 0.0205\ \Omega$, $X_L = 0.1162\ \Omega$, $L_L = 0.1162/(2\pi f) = 0.3082\ mH$

$R_2 = (1/2)\ R_L = 0.01\ \Omega$, $R_{C1} = 500\ \Omega$ $R_{C2} = 500\ \Omega$

(R_{C1} *and* R_{C2} are core loss resistances)

Based on transformer laboratory data, for taps at 10% short circuit test at the transformer secondary, we can average the three results, leading, we average the three results again, leading to:

$V_{SC} = (14.6 + 11.5 + 13.4) / 3 = 13.17\ V$

$I_{SC} = (11.85 + 11.6 + 15.2) / 3 = 12.88\ A$

$R_{1A} = R_{1B} = 0.45 \times R_2 = 0.0045\ \Omega$

$R_{1C} = 0.1 \times R_2 = 0.001\ \Omega$

$L_{LA} = L_{LB} = 0.45\ x\ (1/2) L_L = 0.0693\ mH$

$L_{LC} = 0.1\ x\ (1/2)\ L_L = 0.01541\ mH$

The load are set at: $L_{load3} = 0.045\ mH$ and $R_{load3} = (1/10)\ X_{load3} = 0.0017\ \Omega$.

Since no λ-*i* data is supplied by Dr. Johnson, Mork's λ-*i* [13] is adjusted to determine the *λ-i* data for the nonlinear inductors L_2, L_{1A}, L_{1B}, and L_{1C} such that the rms excitation current of the transformer is approximately 3% of the rated current. Below are the calculations:

$$Z = \omega L = V/I = V^2/S$$

$$Z_{new} / Z_{old} = (V^2_{new} / S_{new}) / (V^2_{old} / S_{old}) = [(240)^2 / 18.33k] / [(7200)^2 / 50k] = 1/330$$

$$L_{new} / L_{old} = Z_{new} / Z_{old} = (\Lambda_{new} / I_{new}) / (\Lambda_{old} / I_{old})$$

$$= [(V_{new} / \omega) / (V_{old} / \omega)] * (I_{old} / I_{new}) = (V_{new} / V_{old}) / (I_{old} / I_{new})$$

$$= (240 / 7200) * (I_{old} / I_{new}) = (1/30)(I_{old} / I_{new}) = 1/330$$

$$I_{new} = (330/30)\ I_{old} = 11\ I_{old}$$

$$\Lambda_{old} / \Lambda_{new} = V_{old} / V_{new} = 7200/240 = 30$$

Thus we have $\lambda_{240} = (1/30)\ \lambda_{7200}$, and $i_{240} = 11 i_{7200}$

Table 3.4 provides input data for taps at 100% short circuit test at the transformer secondary based on the laboratory test data and Mork's *λ-i* data [13]. Table 3.5 provides input data for taps at 10% short circuit test at the transformer secondary based on the laboratory test data and Mork's *λ-i* data [13], the distribution of the segments are 45%, 45%, and 10%.

The tested laboratory transformer was simulated, using the revised duality model (Fig. 20), and the results are described in Test Case 7 through 9.

Table 3.4 DATA FOR REVISED DUALITY-DERIVED MODEL FOR TAPS AT 100% SHORT CIRCUIT TEST AT TRANSFORER SECONDARY BASED ON LABORATORY TEST DATA (Voltage *v* in V, current *i* in A, resistance R in Ω, and inductance L in mH)

Single Phase Transformer		**240 : 240V**	**18.33 KVA**	
v_1 = 10.99(peak)	L_{Load1} = 0.00001	R_{1A} = 0.0033	R_{C1} = 500	L_L = 0. 3082
R_{Load1} = 0.00001	L_{Load2} = 0.00001	R_{1B} = 0.0033	R_{C2} = 500	L_{LA} = 0.0514
R_{Load2} = 0.00001	L_{Load3} = 0.00001	R_{1C} = 0.0033	R_2= 0.01	L_{LB} = 0.0514
R_{Load3} = 0.00001			K = 1	L_{LC} = 0.0514
N_{1A}:N_1	N_{1B}:N_1	N_{1C}:N_1	N_1:N_2	
1:3	1:3	1:3	1:1	
	For L_2	For L_{1A}	For L_{1B}	For L_{1C}
λ_1 (Wbt)	i_{L2} (A)	i_{1A} (A)	i_{1B} (A)	i_{1C} (A)
0.1508	0.0910195	0.030339833	0.030339833	0.030339833
0.3032	0.09295	0.030983333	0.030983333	0.030983333
0.3788	0.1393535	0.046451167	0.046451167	0.046451167
0.451	0.216073	0.072024333	0.072024333	0.072024333
0.49	0.2579005	0.085966833	0.085966833	0.085966833
0.5252	0.334048	0.111349333	0.111349333	0.111349333
0.5626	0.3893175	0.1297725	0.1297725	0.1297725
0.6018	0.528671	0.176223667	0.176223667	0.176223667
0.6384	0.749177	0.249725667	0.249725667	0.249725667
0.6768	1.0582	0.352733333	0.352733333	0.352733333
0.715	1.435291	0.478430333	0.478430333	0.478430333
0.7502	1.837121	0.612373667	0.612373667	0.612373667
0.8268	3.02588	1.008626667	1.008626667	1.008626667
0.9004	6.027307	2.009102333	2.009102333	2.009102333

Table 3.5 DATA FOR REVISED DUALITY-DERIVED MODEL FOR TAPS AT 10% SHORT CIRCUIT TEST AT TRANSFORER SECONDARY BASED ON LABORATORY TEST DATA (Voltage *v* in V, current *i* in A, resistance R in Ω, and inductance L in mH)

Single Phase Transformer		**240 : 240V**	**18.33 KVA**	
$v_1 = 18.63(peak)$	$L_{Load1} = 1$	$R_{1A} = 0.0045$	$R_{C1} = 500$	$L_L = 0.3082$
$R_{Load1} = 1000$	$L_{Load2} = 1$	$R_{1B} = 0.0045$	$R_{C2} = 500$	$L_{LA} = 0.0693$
$R_{Load2} = 1000$	$L_{Load3} = 0.0045$	$R_{1C} = 0.001$	$R_2 = 0.01$	$L_{LB} = 0.0693$
$R_{Load3} = 0.0017$			$K = 1$	$L_{LC} = 0.0154$
$N_{1A}:N_1$	$N_{1B}:N_1$	$N_{1C}:N_1$	$N_1:N_2$	
22.5:50	22.5:50	5:50	50:50	
	For L_2	For L_{1A}	For L_{1B}	For L_{1C}
λ_1 (Wbt)	i_{L2} (A)	i_{1A} (A)	i_{1B} (A)	i_{1C} (A)
0.1508	0.0910195	0.040958775	0.040958775	0.00910195
0.3032	0.09295	0.0418275	0.0418275	0.009295
0.3788	0.1393535	0.062709075	0.062709075	0.01393535
0.451	0.216073	0.09723285	0.09723285	0.0216073
0.49	0.2579005	0.116055225	0.116055225	0.02579005
0.5252	0.334048	0.1503216	0.1503216	0.0334048
0.5626	0.3893175	0.175192875	0.175192875	0.03893175
0.6018	0.528671	0.23790195	0.23790195	0.0528671
0.6384	0.749177	0.33712965	0.33712965	0.0749177
0.6768	1.0582	0.47619	0.47619	0.10582
0.715	1.435291	0.64588095	0.64588095	0.1435291
0.7502	1.837121	0.82670445	0.82670445	0.1837121
0.8268	3.02588	1.361646	1.361646	0.302588
0.9004	6.027307	2.71228815	2.71228815	0.6027307

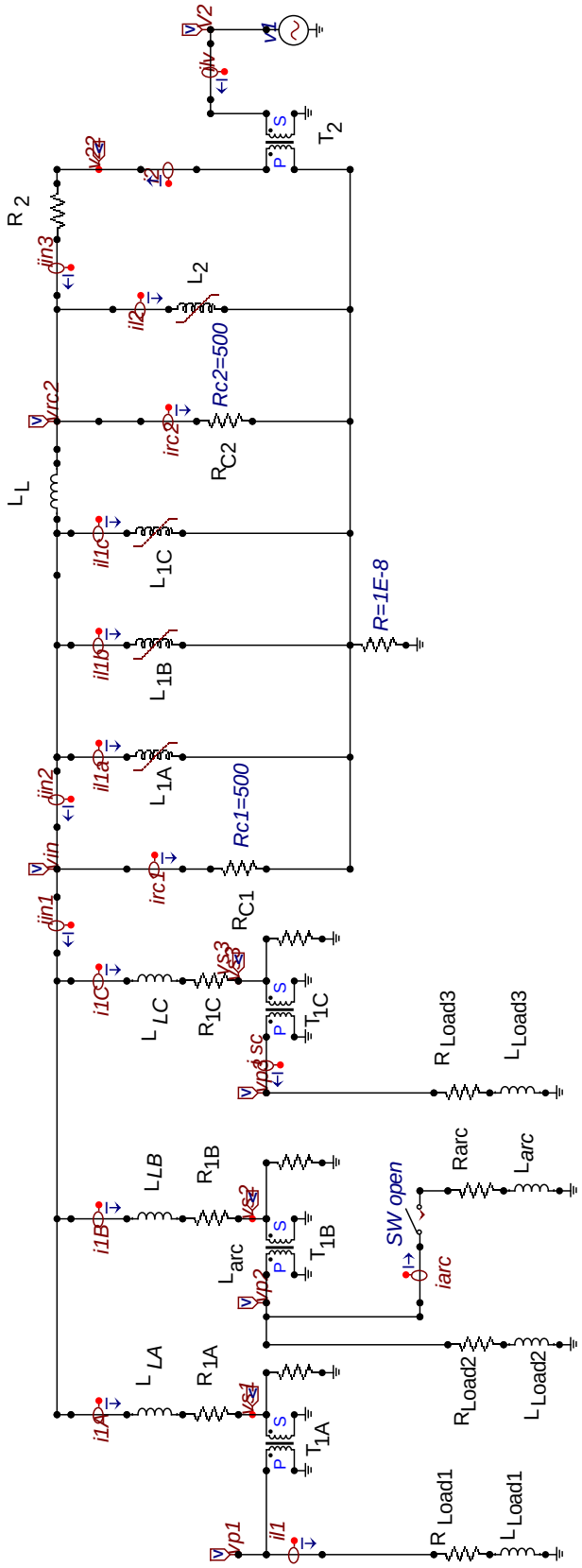

Fig. 20 The revised duality-derived ATP model for single-phase transformer inter-turn fault

Test Case 7 simulates taps at 100% short circuit laboratory test at transformer secondary.

Fig. 27 shows the short-circuit test input voltage waveform and Fig. 28 shows the short-circuit test input current waveform. The applied voltage is 7.77 V RMS. The peak value of the short-circuit test input current is $I_{sc} = 94.2\ A$, $I_{sc\_rms} = 94.2/\sqrt{2} = 66.61A$, which is equivalent to $I_{sc} = 66.61\ x\ \sqrt{3} = 115.3\ A$ of the line current of the delta-connected primary windings. Compare with transformer short circuit laboratory test data, the error is 1.25%.

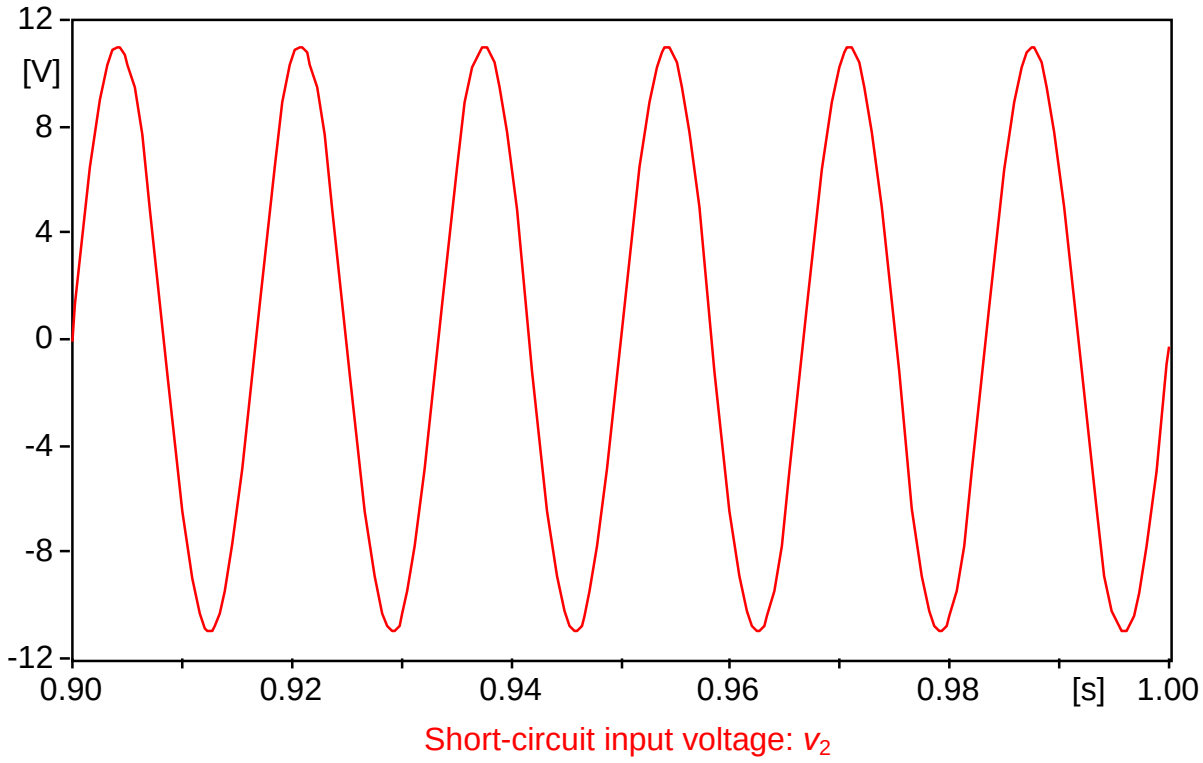

Fig. 27 Taps at 100% Short Circuit Test Input Voltage v_2 Waveform

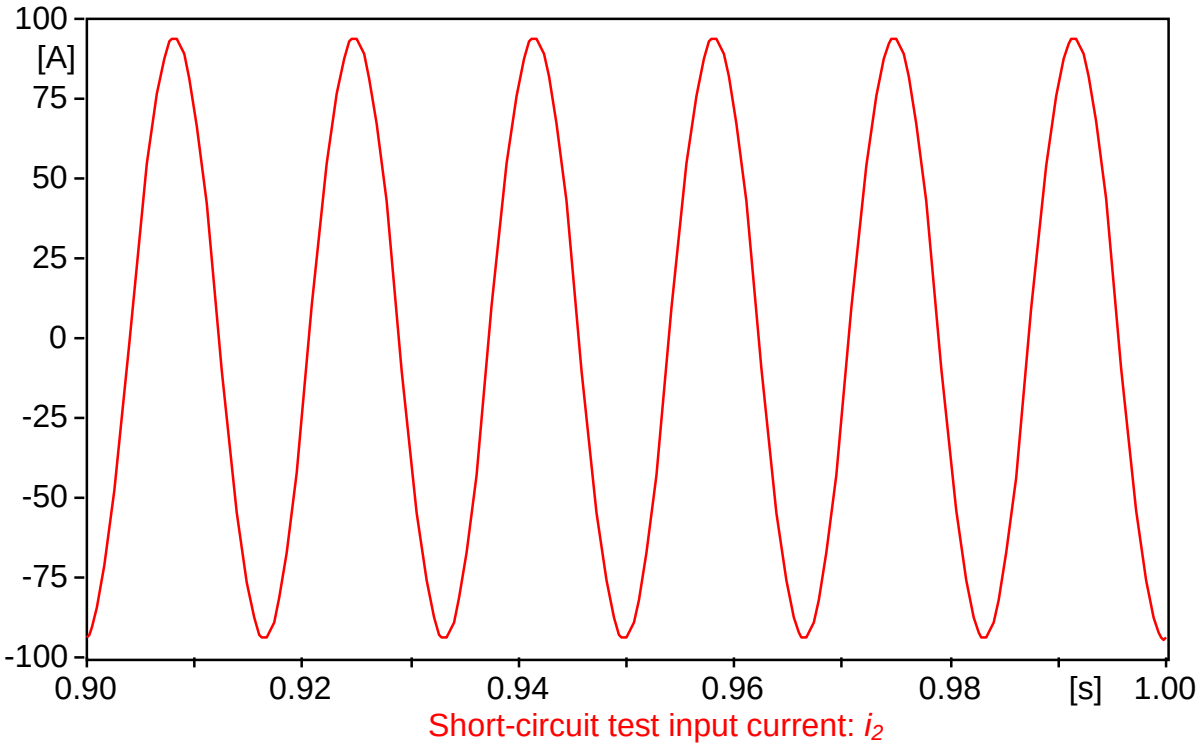

Fig. 28 Taps at 100% Short Circuit Test Input Current i_2 Waveform

Test Case 8 simulates taps at 10% short circuit laboratory test at transformer secondary. Fig. 29 shows the short-circuit test input current waveform. The peak value of the short-circuit test input current or no load current is $I_{sc} = 10.26$ *A*, $I_{sc\_rms} = 10.26 / \sqrt{2} = 7.25$ *A*, which is equivalent to $I_{sc} = 7.25 \times \sqrt{3} = 12.57$*A*. Compare with transformer short circuit laboratory test data, the error is 2.4% of the line current of the delta-connected primary winding.

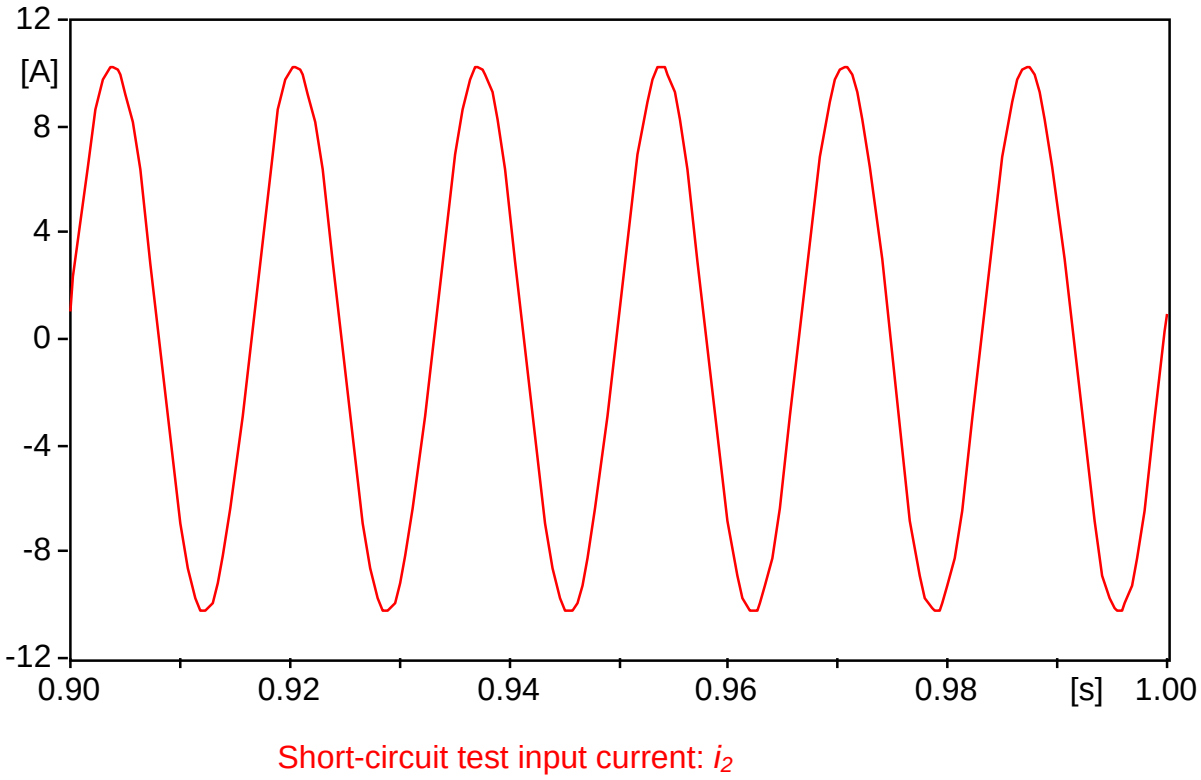

Fig. 29 Taps at 10% Short Circuit Test Input Current i_2 Waveform

Test Case 9 simulates taps at 100% open circuit laboratory test at transformer secondary.

Fig. 30 shows the open circuit test input voltage waveform and Fig. 31 shows the open circuit test input current waveform. The RMS value of the open circuit input current is 5.6 *A*, which is equivalent to $I_{oc} = 5.6 \times \sqrt{3} = 9.7\ A$. Compare with transformer open circuit laboratory test data, the percent error is 2.7.

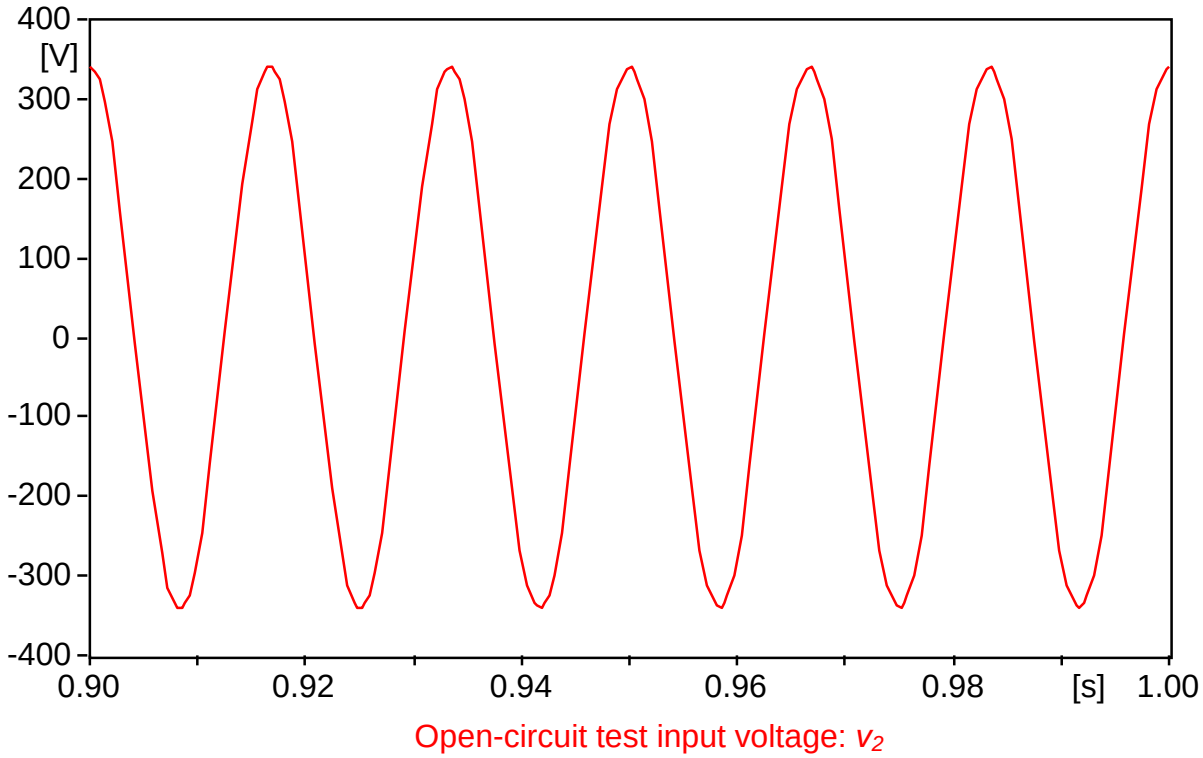

Fig. 30 Taps at 100% Open Circuit Test Input Voltage v_2 Waveform

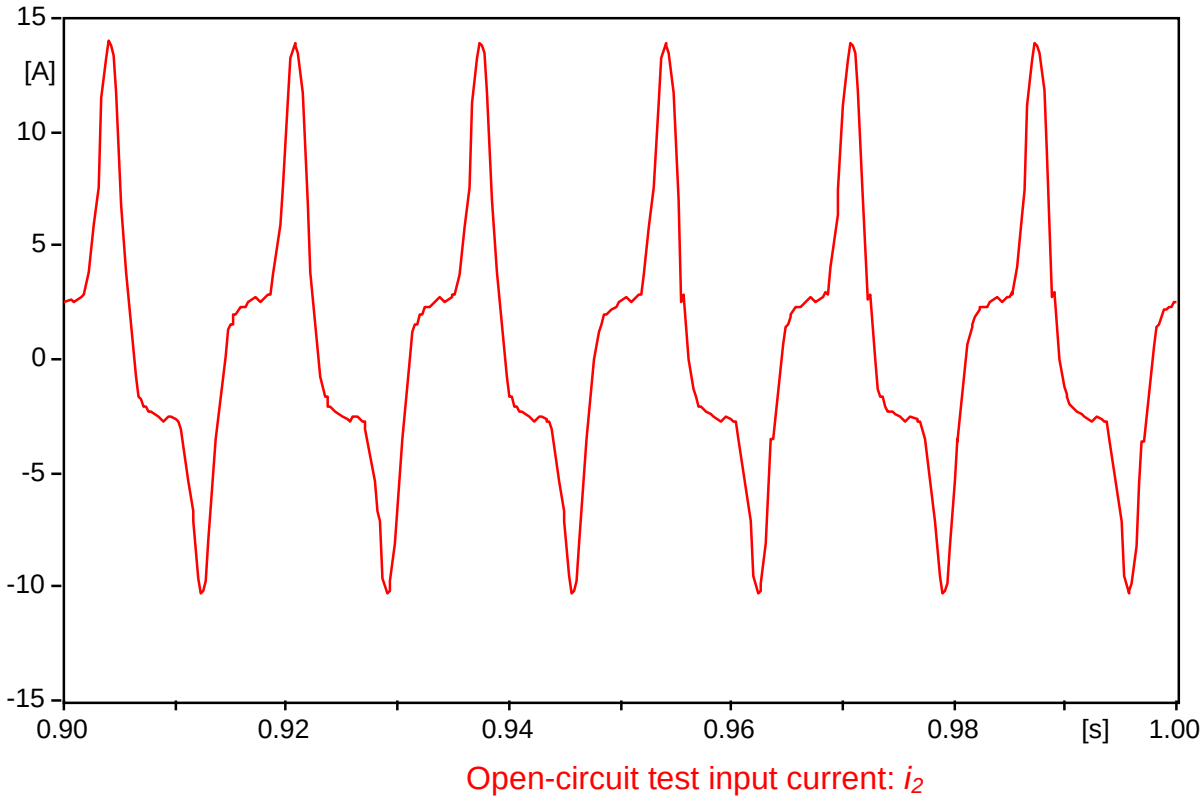

Fig. 31 Taps at 100% Open Circuit Test Input Current i_2 Waveform

The transformer laboratory tests for taps at 5% and 2% short circuit tests are also simulated by the revised duality model. The errors are 2.8% and 3.2%, respectively. Thus the revised duality model for single-phase transformer inter-turn fault is verified by simulating the transformer laboratory tests.

CHAPTER 4: DIRECT SOLUTION OF THE TWO-WINDING, SHELL-TYPE, SINGLE-PHASE TRANSFORMER WITH AN INTER-TURN FAULTS

In this chapter, the solution of the transformer inter-turn fault by using the basic circuit theory is explored. This derivation eliminates the software dependency of the solution of transformer inter-turn fault. Since the devices based on field programmable gate arrays (FPGAs) are used in the field, this derivation might find its use in developing new transformer diagnostic and relay protection schemes.

Fig. 32 shows the equivalent electric circuit of the two-winding, shell-type, single-phase transformer with an inter-turn fault on winding 1. The inter-turn fault is represented by nonlinear resistance R_{arc} and nonlinear inductance L_{arc}.

The differential equations for Fig. 32 can be written:

$$\begin{cases} v_1 = R_{AC} i_1 + \dfrac{d\lambda_{AC}}{dt} + R_{arc}\, i_{arc} + \dfrac{d\lambda_{arc}}{dt} & (11a) \\ R_{1B} i_{1B} + \dfrac{d\lambda_{1B}}{dt} = R_{arc}\, i_{arc} + \dfrac{d\lambda_{arc}}{dt} & (11b) \\ -R_2 i_2 - \dfrac{d\lambda_2}{dt} + L_{L2}\, \dfrac{di_2}{dt} + R_{L2} i_2 = 0 & (11c) \end{cases}$$

Where

$$R_{AC} = R_{1A} + R_{1C} \quad (12a)$$

$$\lambda_{AC} = \lambda_{1A} + \lambda_{1C} \quad (12b)$$

$$i_{1B} = i_1 - i_{arc} \quad (12c)$$

$$\lambda'_{AC} = \lambda_{AC} + \lambda_{arc} \quad (12d)$$

$$\lambda'_{1B} = \lambda_{1B} - \lambda_{arc} \quad (12e)$$

$$\lambda'_2 = \lambda_2 - L_{L2} i_2 \quad (12f)$$

$$i_{arc} = f(\lambda_{arc}) \quad (12g)$$

Substituting Eq. (11) into Eq. (12) results in Eq. (13):

$$\begin{cases} \dfrac{d\lambda'_{AC}}{dt} = -R_{AC} i_1 - R_{arc}\, i_{arc} + v_1 & (13a) \\ \dfrac{d\lambda'_{1B}}{dt} = -R_{1B} i_1 + (R_{1B} + R_{arc})\, i_{arc} & (13b) \\ \dfrac{d\lambda'_{2}}{dt} = (R_{L2} - R_2)\, i_2 & (13c) \end{cases}$$

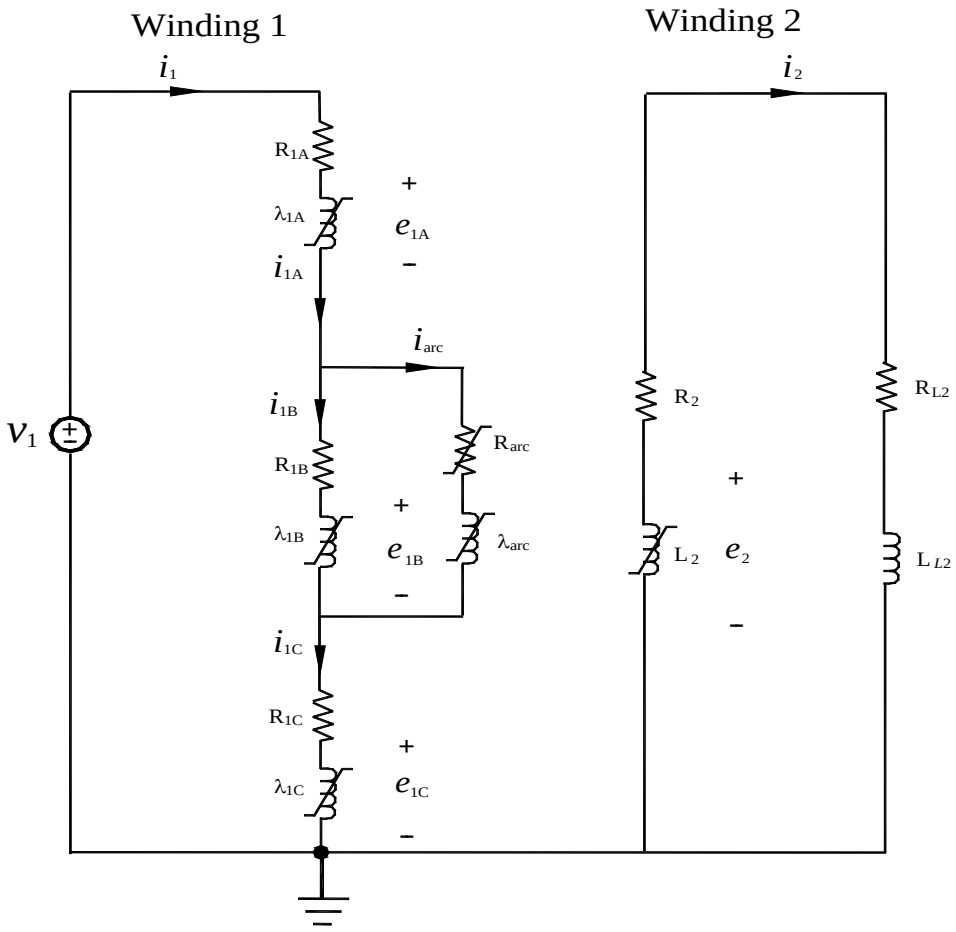

Fig. 32 The equivalent electrical circuit of the two-winding, shell-type, single-phase transformer with an inter-turn fault on winding 1.

In Eq. (13), the state variables are: λ'_{AC} , λ'_{1B} , and λ'_2 , and dependent variables are i_1, i_{arc}, and i_2. Eq. (13) together with Eq. (12) can be solved using trapezoidal rule or other integration formulas. Currents $i_1 = i_{1A} = i_{1C}$, and i_2 can be found from the equivalent magnetic circuit of the transformer which is shown in Fig. 33. Since the core reluctances R_{1A}, R_{1B}, R_{1C}, and R_2 are nonlinear, the circuit can only be solved by an iterative method. From Fig. 33, currents i_1, i_{1B}, and i_2 can be solved from the flux sources ϕ_{1A}, ϕ_{1B}, ϕ_{1C}, and ϕ_2 once the reluctances are known.

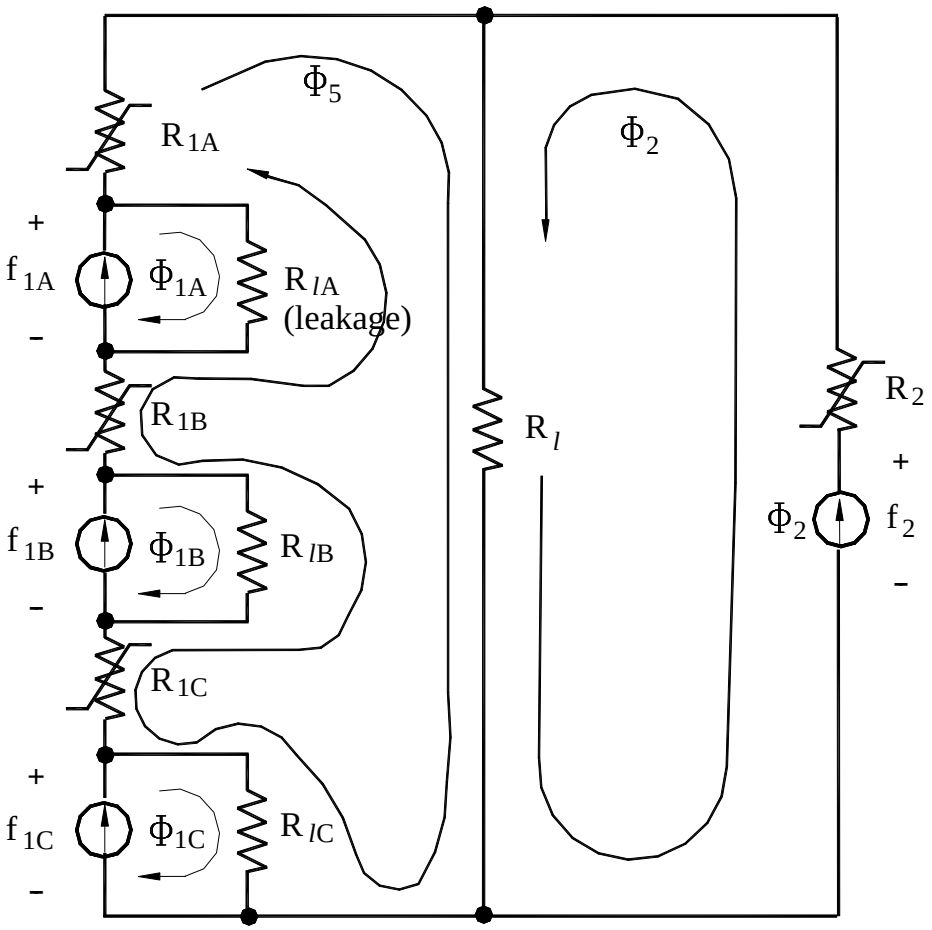

Fig. 33 Magnetic circuit with an inter-turn fault with flux sources and loop fluxes.

If the magnetic circuit of Fig. 32 can be assumed linear, then we can write up loop equations which relate the loop fluxes to the magnetomotive forces as follows:

$$\begin{bmatrix} R_{11} & 0 & 0 & 0 & R_{15} \\ 0 & R_{22} & 0 & 0 & R_{25} \\ 0 & 0 & R_{33} & 0 & R_{35} \\ 0 & 0 & 0 & R_{44} & R_{45} \\ R_{51} & R_{52} & R_{53} & R_{54} & R_{55} \end{bmatrix} \begin{bmatrix} \phi_{1A} \\ \phi_{1B} \\ \phi_{1C} \\ \phi_2 \\ \phi_5 \end{bmatrix} = \begin{bmatrix} f_{1A} \\ f_{1B} \\ f_{1C} \\ f_2 \\ 0 \end{bmatrix} = \begin{bmatrix} N_{1A} i_{1A} \\ N_{1B} i_{1B} \\ N_{1C} i_{1C} \\ N_2 i_2 \\ 0 \end{bmatrix} \qquad (14)$$

ϕ_{1A} ϕ_{1B} ϕ_{1C} ϕ_2 ϕ_5

$R_{11} = R_{lA}$ $R_{21} = 0$
$R_{12} = 0$ $R_{22} = R_{lB}$
$R_{13} = 0$ $R_{23} = 0$
$R_{14} = 0$ $R_{24} = 0$
$R_{15} = - R_{lA}$ $R_{25} = - R_{lB}$

$R_{31} = 0$ $R_{41} = 0$
$R_{32} = 0$ $R_{42} = 0$
$R_{33} = R_{lC}$ $R_{43} = 0$
$R_{34} = 0$ $R_{44} = R_2 + R_l$
$R_{35} = - R_{lC}$ $R_{45} = R_l$

$R_{51} = - R_{lA}$
$R_{52} = - R_{lB}$
$R_{53} = - R_{lC}$
$R_{54} = R_l$
$R_{55} = R_{1A} + R_{1B} + R_{1C} + R_{lA} + R_{lB} + R_{lC} + R_l$

Eq. (14) relates the 5 loop fluxes to the 4 externally applied mmfs. The objective is to relate the 4 winding fluxes (which are equal to the first 4 loop fluxes), to the 4 applied mmfs. This can be done by solving flux ϕ_5 from the last equation of Eq. (14) and substituting it into the first 4 equations.

Mathematically, Eq. (14) is of the pattern

$$\begin{bmatrix} \mathbf{A}_{11} & \boldsymbol{A}_{12} \\ \boldsymbol{A}_{21} & \boldsymbol{A}_{22} \end{bmatrix} \begin{bmatrix} \boldsymbol{\phi}_{\mathrm{I}} \\ \boldsymbol{\phi}_{\mathrm{II}} \end{bmatrix} = \begin{bmatrix} \mathbf{f} \\ \mathbf{0} \end{bmatrix} \qquad \text{A-t} \qquad (15)$$

Or

$$\boldsymbol{A}_{11}\,\boldsymbol{\phi}_I + \boldsymbol{A}_{12}\,\boldsymbol{\phi}_{II} = \boldsymbol{f} \qquad \text{A-t} \qquad (16a)$$

$$\boldsymbol{A}_{21}\,\boldsymbol{\phi}_I + \boldsymbol{A}_{22}\,\boldsymbol{\phi}_{II} = \boldsymbol{0} \qquad \text{A-t} \qquad (16b)$$

Solving $\boldsymbol{\phi}_{\mathrm{II}}$ from Eq. (16b) and substituting it into Eq. (16a) results in

$$\boldsymbol{A}_{11}\,\boldsymbol{\phi}_I + \boldsymbol{A}_{12}\,(-\boldsymbol{A}_{22}^{-1}\,\boldsymbol{A}_{21})\,\boldsymbol{\phi}_I = (\boldsymbol{A}_{11} - \boldsymbol{A}_{12}\,\boldsymbol{A}_{22}^{-1}\,\boldsymbol{A}_{21})\,\boldsymbol{\phi}_I = \boldsymbol{f} \qquad \text{A-t} \qquad (17)$$

$$R = A_{11} - A_{12}\,A_{22}^{-1}\,A_{21}$$

$$\boldsymbol{\phi}_{II} = (-\boldsymbol{A}_{22}^{-1}\,\boldsymbol{A}_{21})\,\boldsymbol{\phi}_I \qquad (18)$$

Completing the computation results in

$$\boldsymbol{R} = \begin{bmatrix} R_{11} & 0 & 0 & 0 \\ 0 & R_{22} & 0 & 0 \\ 0 & 0 & R_{33} & 0 \\ 0 & 0 & 0 & R_{44} \end{bmatrix} - \begin{bmatrix} R_{15} \\ R_{25} \\ R_{35} \\ R_{45} \end{bmatrix} (1/R_{55}) \begin{bmatrix} R_{51} & R_{52} & R_{53} & R_{54} \end{bmatrix}$$

$$= \begin{bmatrix} R_{11} & 0 & 0 & 0 \\ 0 & R_{22} & 0 & 0 \\ 0 & 0 & R_{33} & 0 \\ 0 & 0 & 0 & R_{44} \end{bmatrix} - (1/R_{55}) \begin{bmatrix} R_{15}R_{51} & R_{15}R_{52} & R_{15}R_{53} & R_{15}R_{54} \\ R_{25}R_{51} & R_{25}R_{52} & R_{25}R_{53} & R_{25}R_{54} \\ R_{35}R_{51} & R_{35}R_{52} & R_{35}R_{53} & R_{35}R_{54} \\ R_{45}R_{51} & R_{45}R_{52} & R_{45}R_{53} & R_{45}R_{54} \end{bmatrix} \qquad (19)$$

It is noted that in per unit, $\boldsymbol{R} = \boldsymbol{\Gamma}$, the inverse inductance matrix.

Eq. (14) is only valid for linear circuits. When nonlinearity is considered, core saturation etc., Eq. (14) is not valid for the magnetic circuit of Fig. 33. The reason for this is that although the flux sources at each step are known, the fluxes flowing in the 4 nonlinear reluctances are unknown, therefore, the values of the nonlinear reluctances are unknown at that step. So the reluctances matrix $\boldsymbol{R}$ is not valid. If the three leakage reluctances R_{l1}, R_{l2}, and R_{l3} are omitted, every time when flux sources ϕ_{1A}, ϕ_{1B}, and ϕ_{1C} are known, then the reluctances R_{lA}, R_{lB}, and R_{lC} are known, and the reluctance matrix is valid. To solve the nonlinear magnetic circuit accurately, the Newton-Raphson discrete circuit method can be used.

CHAPTER 5: SOLVING THE TWO-WINDING, SHELL-TYPE, SINGLE-PHASE TRANSFORMER WITH INTER-TURN FAULTS USING PSPICE

In Chapter 5, the solution of the transformer inter-turn fault using PSPICE (Personal Simulation Program with Integrated Circuit Emphasis) to solve the coupled electric and magnetic circuits simultaneously is explored.

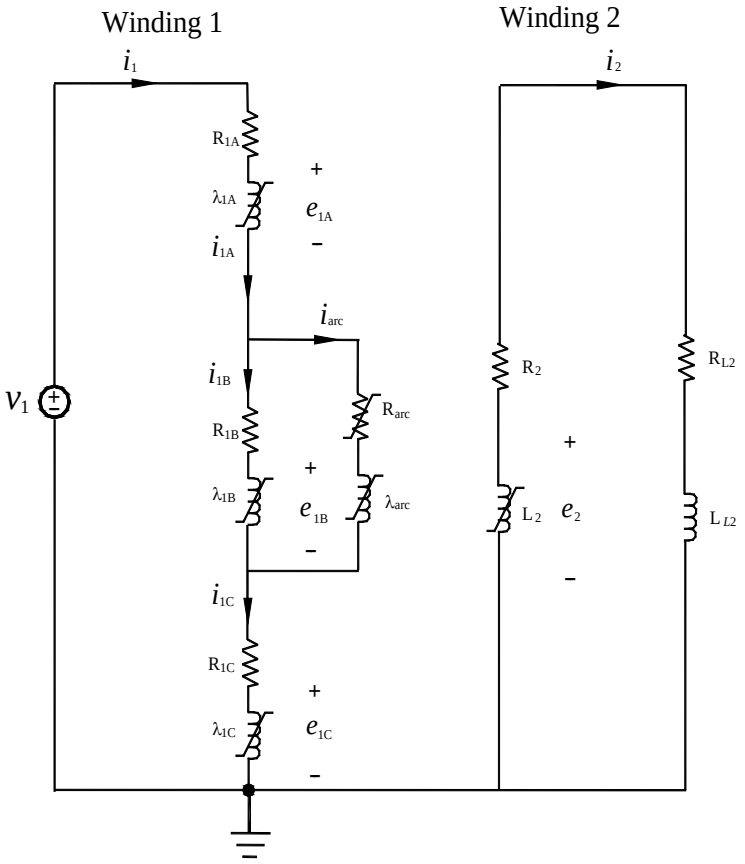

Fig. 32 The equivalent electrical circuit of the two-winding, shell-type, single-phase transformer with an inter-turn fault on winding 1.

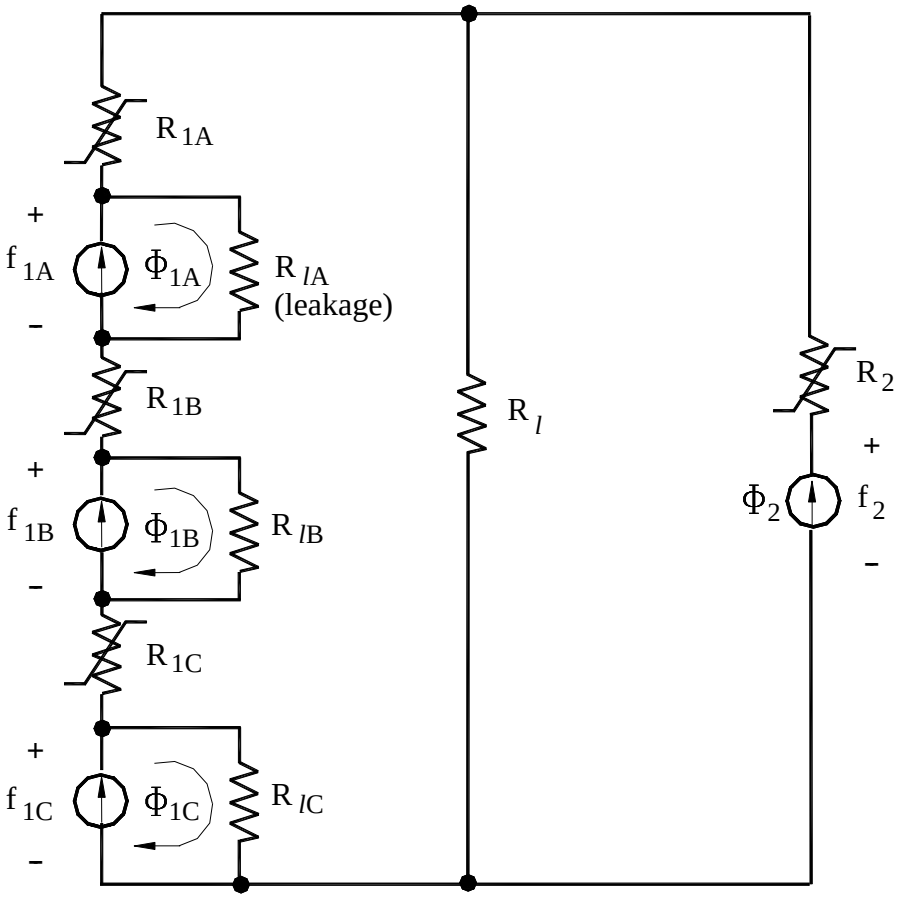

Fig. 34 Magnetic circuit with an inter-turn fault showing flux sources.

The induced voltages $e_{1A} = \frac{d\lambda_{1A}}{dt}$, $e_{1B} = \frac{d\lambda_{1B}}{dt}$, and $e_{1C} = \frac{d\lambda_{1C}}{dt}$ in Fig. 32 of chapter 4 are related with their respective winding currents i_{1A}, i_{1B}, and i_{1C} through magnetic induction.

As is shown in Fig. 34, the driving forces in the magnetic circuit are the three flux sources ϕ_{1A}, ϕ_{1B}, ϕ_{1C} (magnetomotive forces $f_{1A} = N_{1A}\, i_{1A}$, $f_{1B} = N_{1B}\, i_{1B}$, $f_{1C} = N_{1C}\, i_{1C,}$ and $f_2 = N_2\, i_2$ can also be used, if one likes to use them). R_{1A}, R_{1B}, and R_{1C} are core reluctances of winding 1 segments. R_{lA}, R_{lB}, and R_{lC} are leakage reluctances of the winding 1 segments. R_2 is the core reluctance of winding 2 and R_l is the leakage reluctance between winding 1 and winding 2.

Fig. 32 and Fig. 34 can be solved by PSPICE simultaneously. PSPICE Analog Behavioral Models (ABMs) have the integration function SDT(x) and derivative function DDT(x), so that the electric and magnetic circuits can be computed separately but simultaneously.

$SDT\ (v) = \int v\ dt$ (Integration function)

$DDT\ (\lambda) = \frac{d\lambda}{dt} = v$ (Derivative function)

In the instant case, we have

$SDT\ (e_{1A}) = \lambda_{1A} = N_{1A}\,\phi_{1A}$

$DDT\ (\lambda_{1A}) = \frac{d\lambda_{1A}}{dt} = v_{1A}$

SDT integrates the voltage into flux linkage, which is scaled by the winding turns into flux which is the flux source in the magnetic circuit. The computed magnetomotive force across each flux source resulting from the integration function is scaled by the winding turns into current in the electric circuit.

Fig. 35 illustrates PSPICE solution method for a coupled electric and magnetic circuit. Table 3.6 shows the transformer inter-turn fault data for PSPICE model. Fig. 36 shows the PSPICE electric and magnetic circuit models for the single-phase, two-winding transformer inter-turn fault. Fig. 37 shows the PSPICE ABM (Analog Behavioral Modeling) schematics for the model. Fig. 38 shows the electric and magnetic circuits with ABM schematics.

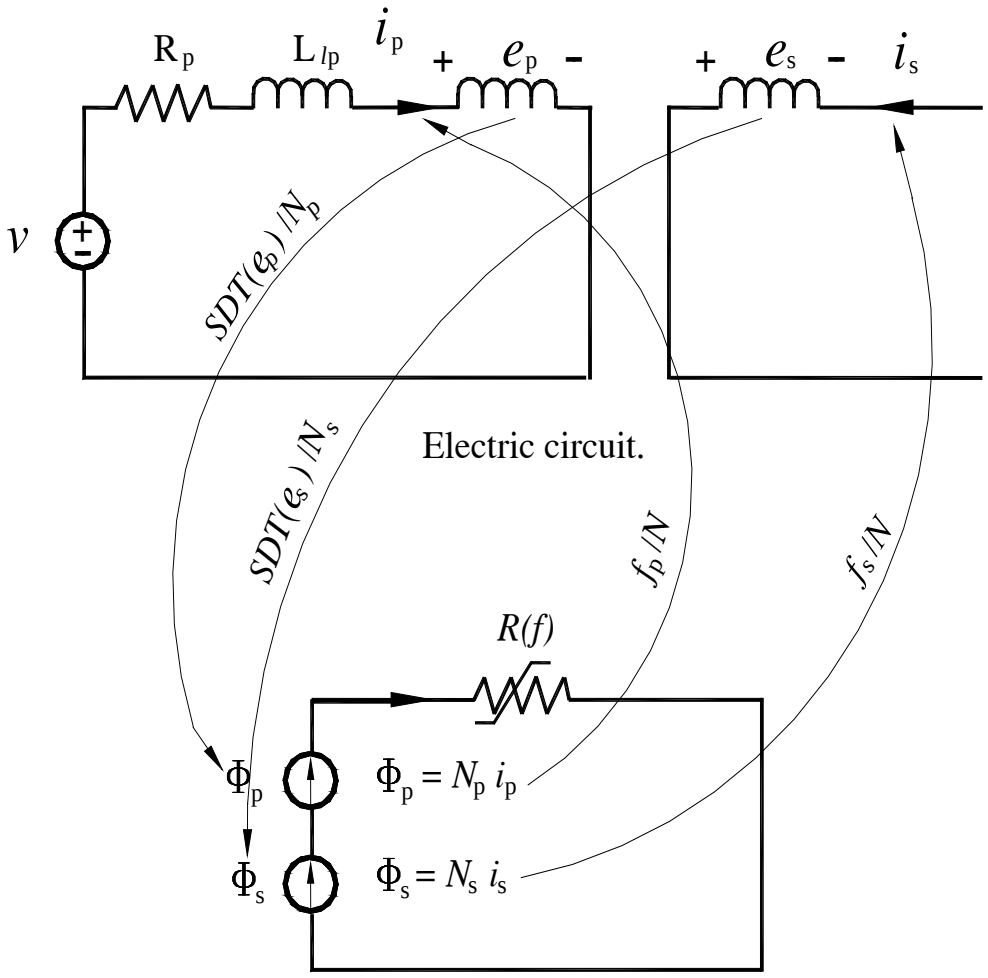

Fig. 35 PSPICE solution method.

Table 3.6 TRANSFORER INTER-TURN FAULT PSPICE MODEL DATA TABLE
(Voltage *v* in V, current *i* in A, resistance R in Ω, and inductance L in mH)

Single Phase Transformer		**7200 : 120V**	**50 KVA**	
v_1 =10182(peak)		$R_{C1} = 10^5$		L_L = 838
R_{Load} = 0.2304		$R_{C2} = 10^5$		L_{LA} = 5.586
L_{Load} = 0. 4584		R_2 = 4.32		L_{LB} = 5.586
R_{1A} = 1.3067		R_{arc} = 9.54		L_{LC} = 5.586
R_{1B} = 1.3067		L_{arc} = 18.98		
R_{1C} = 1.3067		L_2 = 81.12		
$N_{1A}:N_1$	$N_{1B}:N_1$	$N_{1C}:N_1$	$N_1:N_2$ =	
2400:7200	2400:7200	2400:7200	7200:120	
	For $\mathcal{R}_2$	For $\mathcal{R}_{1A}$	For $\mathcal{R}_{1B}$	For $\mathcal{R}_{1C}$
λ_1 (Wbt)	= $(N_2^2 * i_{L2})/\lambda_1$	= $(N_{1A}^2 * i_{1A})/\lambda_1$	= $(N_{1B}^2 * i_{1B})/\lambda_1$	= $(N_{1C}^2 * i_{1C})/\lambda_1$
4.524	33.766578	4502.210433	4502.210433	4502.210433
9.096	17.150396	2286.719437	2286.719437	2286.719437
11.364	20.580781	2744.104189	2744.104189	2744.104189
13.53	26.802661	3573.688101	3573.688101	3573.688101
14.7	29.444898	3925.986395	3925.986395	3925.986395
15.756	35.582635	4744.351358	4744.351358	4744.351358
16.878	38.713118	5161.749022	5161.749022	5161.749022
18.054	49.145896	6552.786086	6552.786086	6552.786086
19.152	65.651629	8753.550543	8753.550543	8753.550543
20.304	87.470449	11662.726556	11662.726556	11662.726556
21.45	112.302098	14973.613054	14973.613054	14973.613054
22.506	136.998134	18266.417844	18266.417844	18266.417844
24.804	204.741171	27298.822771	27298.822771	27298.822771
27.012	374.491337	49932.178291	49932.178291	49932.178291

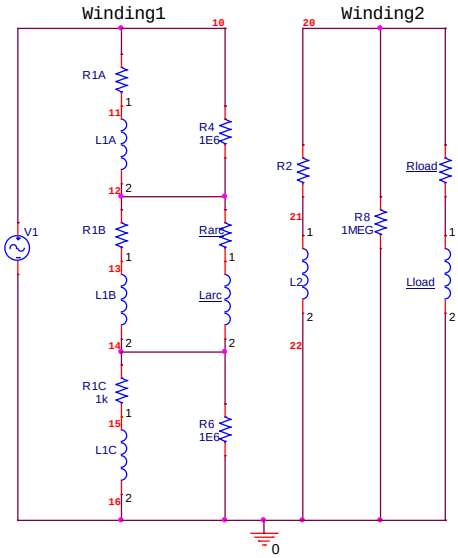

The equivalent electrical circuit of the two-winding,shell-type,single-phase transformer with a inter-turn fault on winding1.

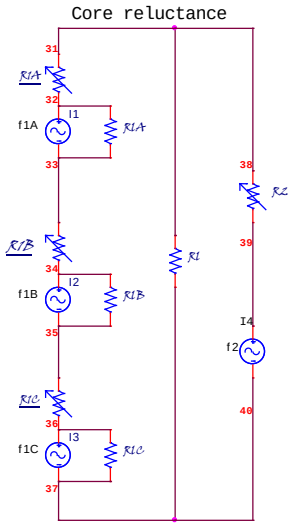

Magnetic circuit of transformer with an inter-turn faults.

Title	PSPICE Model For Transformer 1-Ph Inter-Turn Fault	
Size A	Document Number <Doc>	Rev 0.0.1
Date: Thursday, November 27, 2014	Sheet 1 of 1	

Fig. 36 PSPICE model for single-phase, two-winding transformer inter-turn fault

E	VCVS	Voltage Controlled Voltage Source
F	CCCS	Current Controlled Current Source
G	VCCS	Voltage Controlled Current Source
H	CCVS	Current Controlled Voltage Source

Curve fitting equations for λ-*i* curves :

For $\mathcal{R}_2$: $V_2 = 6E\text{-}06i_2^6 - 0.0004i_2^5 + 0.0105i_2^4 - 0.0968i_2^3 + 0.0678i_2^2 + 2.6377i_2 + 0.0512$

For $\mathcal{R}_{1A}$:$V_{1A} = 5E\text{-}09i_{1A}^6 - 4E\text{-}07i_{1A}^5 + 9E\text{-}06i_{1A}^4 - 8E\text{-}05i_{1A}^3 + 6E\text{-}05i_{1A}^2 + 0.0022i_{1A} + 4E\text{-}05$

For $\mathcal{R}_{1B}$ $V_{1B} = 5E\text{-}09i_{1B}^6 - 4E\text{-}07i_{1B}^5 + 9E\text{-}06i_{1B}^4 - 8E\text{-}05i_{1B}^3 + 6E\text{-}05i_{1B}^2 + 0.0022i_{1B} + 4E\text{-}05$

For $\mathcal{R}_{1C}$:$V_{1C} = 5E\text{-}09i_{1C}^6 - 4E\text{-}07i_{1C}^5 + 9E\text{-}06i_{1C}^4 - 8E\text{-}05i_{1C}^3 + 6E\text{-}05i_{1C}^2 + 0.0022i_{1C} + 4E\text{-}05$

**i = H1A(32,31); V = V1A(31,32)

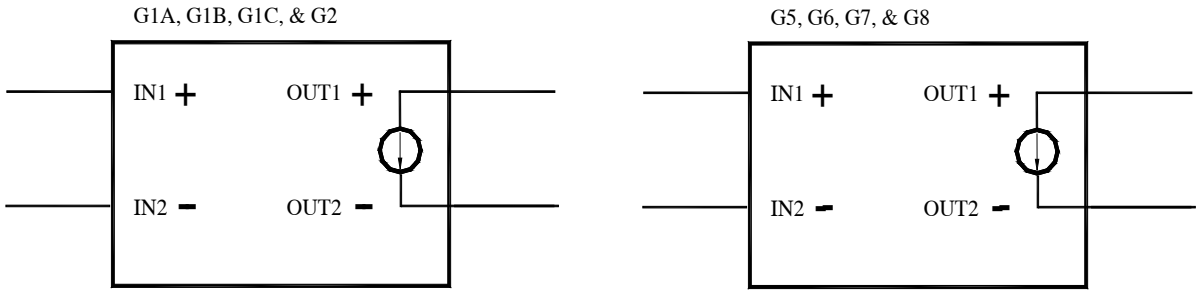

G1A: input = V_{L1A}, output = I_{f1A}
G1B: input = V_{L1B}, output = I_{f1B}
G1C: input = V_{L1C}, output = I_{f1C}
G2: input = V_{L2}, output = I_{f2}

G5: input = V_{f1A}, output = I_{L1A}
G6: input = V_{f1B}, output = I_{L1B}
G7: input = V_{f1C}, output = I_{L1C}
G8: input = V_{f2}, output = I_{L2}

(a) GVALUE schematics

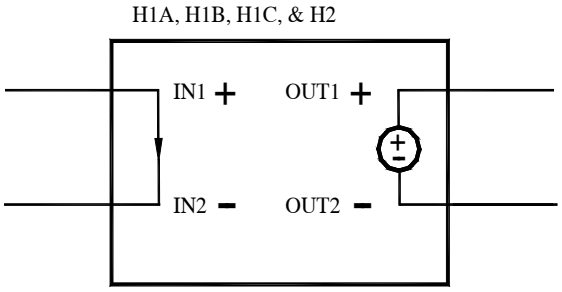

H1A: input = I_{R1A}, out = V_{R1A}
H1B: input = I_{R1B}, out = V_{R1B}
H1A: input = I_{R1C}, out = V_{R1C}
H2: input = I_{R2}, out = V_{R2}

(b) HVALUE schematic

Fig. 37 PSPICE ABM (Analog Be4ehavioral Modeling) schematics

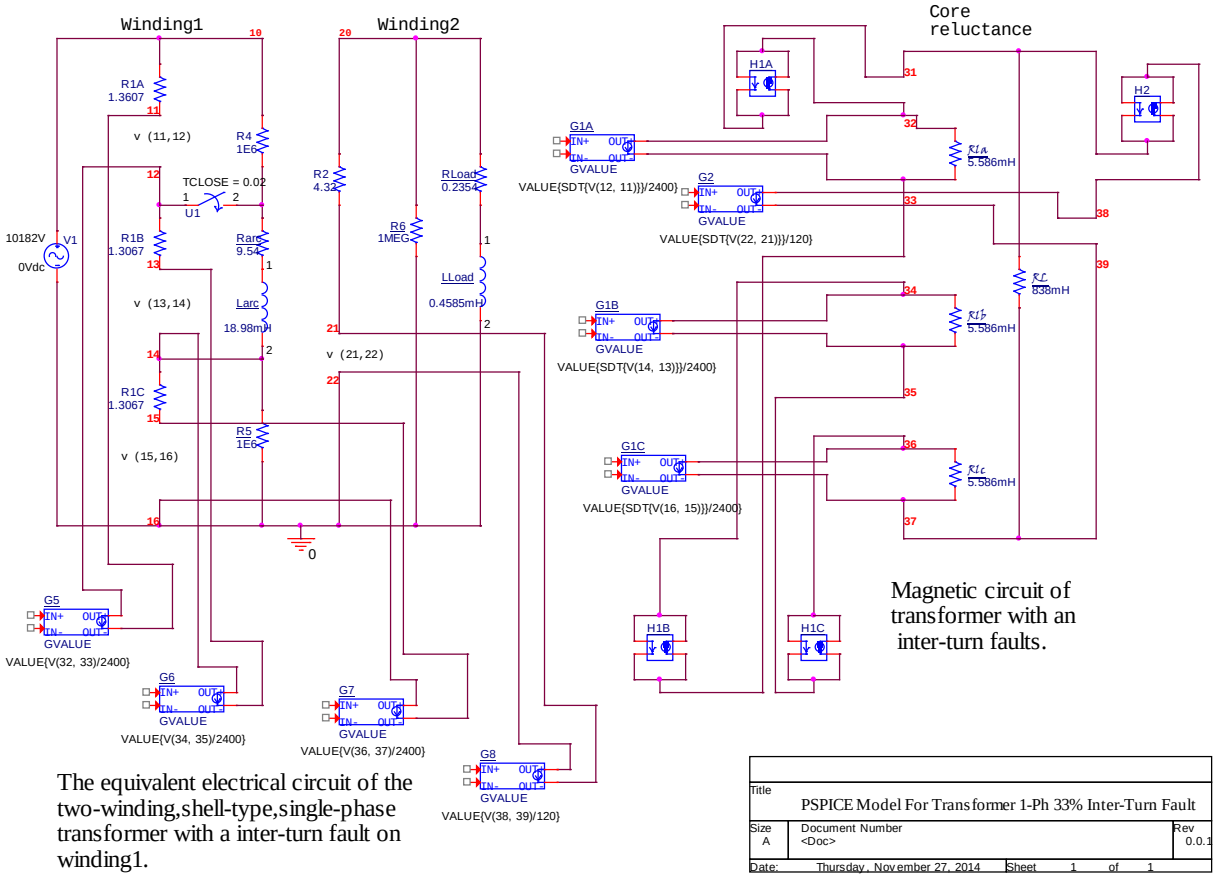

Fig. 38 Full PSPICE model for single-phase, two-winding, Single-phase transformer inter-turn fault with ABM blocks

The model was not able to run due to the limits of the number of components in the student version of PSPICE. The student version cannot handle the complexity of my circuits, but I am very confident about the methodology and correctness of my transformer electric and magnetic circuits. A copy of PSPICE professional version program will be obtained in the future and the studies on this topic will be completed with the PSPICE professional version program.

CHAPTER 6: SUMMARY, CONCLUSIONS, AND FUTURE WORK

Power transformers are important components of the energy transmission and distribution system for electric utilities. Inter-turn winding faults, occurring primarily from turn-to-turn insulation degradation, are one of the leading causes of failures in power transformers. It would be advantageous to detect inter-turn fault in its earliest stage while the transformer is in operation to prevent further damage to the transformer thereby reducing repair cost and transformer outage time.

This thesis reviewed literature on modeling of inter-turn fault and developed a new model. Using duality between magnetic and electric circuits, a topology-based model for two-winding, shell-type, single-phase transformer inter-turn faults was developed. The model is implemented into the Alternative Transients Program (ATP/EMTP) using its circuit components. The model has been validated by simulation of Dr. Johnson's laboratory transformer at no load, short circuit, inrush, and inter-turn faults. The results are convincing. While the developed model is for single-phase transformers, extending it to topology-based, three-phase, three-legged and five-legged transformers are straight forward. Based on basic electric theory, equations for direct solution of the transformer inter-turn fault were also developed. This may find its important usage in transformer relay protection. The thesis discussed using PSPICE for the solution of transformer inter-turn fault as well.

Two important limitations in the ATP/EMTP programs were observed: 1) ATP/EMTP Saturable Transformer Components do not work properly in series and therefore transformer source side winding inter-turn faults cannot be simulated; 2) Even though the Saturable Transformer Components can be connected in series, the voltage ratio equals the turns ratio during the inter-turn fault is not guaranteed.

Future work: possible areas of future work include

- Extending inter-turn fault to model turn to ground faults.
- Extending the model to represent three phase transformers with different core structures.
- Fully develop and refine the Direct Solution Method.
- Fully develop the PSPICE method.

- **REFRENCES**

[1] Patrick Bastard, “A transformer model for winding fault studies,” *IEEE Transactions on Power Delivery*, Vol. 9, No. 2, pp. 690-699, April 1994.

[2] M. Jabloński and E. Napieralska-Juszczak, “Internal Faults in Power Transformer,” *IET Electr. Power Appl.*, Vol. 1, No. 1, January 2007, pp. 105-111.

[3] Luis. M. R. Oliveira and A. J. Marques Cardoso, “A permeance-based transformer model and its application to winding interturn arcing fault studies,” *IEEE Transactions on Power Delivery*, Vol. 25, No. 3, pp. 1589-1598, July 2010.

[4] J. R. Espinoza, “Modeling Transformers with Incipient Faults Using Magnetic circuit.” North American Power Symposium (NAPS), Sept. 9-11, 2012, pp. 1-6.

[5] B. A. Mork, “Transformer Internal Fault Modeling in ATP,” IPST 2011 in Delft, the Netherlands June 14-17, 2011.

[6] H. Wang and d Karen L. Butler, “Modeling Transformers With Internal Incipient Faults,” *IEEE Transactions on Power Delivery*, Vol. 17, No. 2, April 2002, pp. 500-509.

[7] Professor Joe Law and his students, "Transformer testing station: Determining Sensitivity of a Relay to Inter-turn Faults on an Energized Power Transformer," May 2007. Advised by Dr. Joe Law and sponsored by SEL (Schweitzer Engineering Laboratories, Inc.), URL : http://seniordesign.engr.uidaho.edu/2006_2007/teamprotection/docs/tp_slides.ppt
Date accessed: March 16, 2014.

[8] Gordon R. Slemon, *Electric Machines and Drives*, Adison-Wesley Publishing Company, Inc., 1992, pp. 250-251.

[9] X. S. Chen and Paul Neudorfer, “Digital Model for Transient Studies of a Three-phase

Five-Legged Transformer," *IEE Proceedings-C*, Vol. 139, No. 4, 1992, pp. 351-358.

[10] X. S. Chen and S. S. Venkata, "A Three-Phase Three-Winding Core-Type Transformer Model for Low-Frequency Transient Studies," *IEEE Transactions on Power Delivery*, Vol. 12, No. 2, April 1997, pp. 775-782.

[11] X. S. Chen, "A Three-Phase Multi-Legged Transformer Model in ATP Using the Directly-Formed Inverse Inductance Matrix," *IEEE Transactions on Power Delivery*, Vol. 11, No.3, July 1996, pp. 1554-1562.

[12] N. Y. Abed and O. A. Mohammed, "Modeling and characterization of transforms internal faults using finite element and discrete wavelet transformers," *IEEE Trans*. Magn., Vol. 43, No. 4, April 2007, pp. 1425-1428.

[13] Bruce. A. Mork, "Hybrid Transformer Model for Transient Simulation - Part I: Development and Parameters," *IEEE Transactions on Power Delivery*, Vol. 22, No. 1, January 2007, pp. 248-255.

[14] Allan Greenwood, *Electrical Transients in Power System*, 2nd edition, pp. 426-428.